Sufficient Conditions for the Suboptimality of Identical Quantizer Distributed Detection

Prepared by Chin-Yen Yang

National Chiao Tung University

Hsinchu, Taiwan 300, R.O.C.

E-mail: kururu108.cm96@g2.nctu.edu.tw

July, 2012

摘要

在設計最佳分散式偵測系統的挑戰之一，就是可能的設計組合會隨著偵測器的個數增加而成指數成長。反之，找出最佳的同化量化器系統設計(Identical Quantizer System or IQS)是比較容易的，因爲可能的組合是隨著偵測器的個數呈線性成長。因此衍生一個在此領域很重要的研究課題，就是在什麼條件下，最佳的同化量化器系統(IQS)可達到最佳分散式偵測系統設計的效能？

在這篇碩士論文中，我們嘗試用不同的方式思考此一問題：在什麼條件下，IQS僅能達到次佳的整體效能。運用參考論文[4]中的推導方式，我們比較了同化量化器系統設計(IQS)和只改變一個偵測器量化方式的非同化量化器系統設計(Non-identical Quantizer System or NQS)的錯誤率，然後理論證明出在局部觀察值的機率符合某些特定的線段區域條件，IQS僅能達到次佳的效能。我們同樣也嘗試運用數值模擬的方式，來驗證同化量化器系統設計(IQS)僅能達到次佳效能的區域，結果顯示我們的方法應可再推廣至更多的區段。

Abstract

One engineering challenge in designing an optimal distributed detection system is that the number of all possible designs (i.e., the combinations of local likelihood-ratio quantizers (LRQs) and the fusion rule) grows exponentially with the number of local sensors. Instead, finding the best identical quantizer design is a much easier task because the number of possibilities only increase linearly with the number of sensors. This then arises the long-standing query on the condition under which the best identical quantizer system (IQS) is also globally optimal.

In this thesis, we try to revisit the same query by asking a different but related question: when the IQS is only suboptimal. Using the technique in [4], we compare the performances between the best IQS and the NQS with one different local quantizer, and determine theoretically a few line regions that give affirmative answer to our question. We also numerically identify certain regions that make the best IQS only suboptimal. Observations on patterns of these regions are subsequently made and remarked.

Acknowledgements

I would like to show my gratitude to my advisor, Professor Po-Ning Chen, for his patient guidance and support. I would also like to express my appreciation to Professor Peng-Hua Wang for his precious commands in my research. This thesis would not have been possible without these helps. Besides, I would like to thank two lab seniors, Yi-Hong Yang and Ting-Yi Wu, for their advices on my research, particularly for their help in resolving the problems on LaTex. Finally, I really appreciate the support and friendship from all the members in the NTL lab in these two years.

Contents

List of Figures

Chapter 1

Introduction

In this thesis, the parallel distributed detection problem [1–5] defined below is studied.

Consider a distributed detection system consisting of n geographically dispersed sensors and a fusion center, in which the ith sensor receives an observation Y_i drawn possibly from one of the two hypothesis distributions. Upon its reception, the observation Y_i is quantized into an m-ary data $U_i = f(Y_i)$, which is then sent to the fusion center. Afterwards, the fusion center performs binary hypothesis testing based on the received data $(U_1, \ldots, U_n)$, and determine which of the two hypotheses, H_0 or H_1, is the truly happening one.

In its practice, it is more engineeringly convenient to quantize each Y_i by the same quantization rule, which is usually termed the *identical quantizer system*. However, it is known that such an identical quantizer system design is sometimes only suboptimal in detection error, and the optimal design mostly adopts *non-identical quantizers*. Hence, it is of theoretical interest to investigate when the simple identical quantizer system yields the optimal performance. It is however hard to prove the global optimality of the simple identical quantizer system. On the contrary, we turn to investigate under which condition the non-identical quantizer system design strictly outperforms the best identical quantizer system in this thesis.

In notations, we denote the detection error of the optimal (possibly non-identical) distributed detection system by $\gamma^*(\pi)$, and use $\gamma^\diamond(\pi)$ to denote the detection error of the best identical quantizer system, where π is the prior probability of the null hypothesis H_0. We will study what distribution of local observation Y_i will give

$$\gamma^*(\pi) < \gamma^\diamond(\pi).$$

In the literature, only few publications have been devoted to this theoretical problem. The study of our thesis is basically a followup work of [1]. In summary, this publication [1] first pointed out a known result from [2] that even if the local observations $Y_1, \ldots, Y_n$ are *independent and identically distributed* (i.i.d.), the optimal quantizers are not necessarily identical. It then proved the conjecture in [3] that the boundedness assumption in local statistics can be removed. It then proceeded to show that under certain boundedness condition, the ratio $\gamma^*(\pi)/\gamma^\diamond(\pi)$ is asymptotically bounded from below. The authors in [1] also showed that the conjecture that the ratio $\gamma^*(\pi)/\gamma^\diamond(\pi)$ approaches one as the number of sensors n goes to infinity is in general not true. Another publication of the same authors [4] provided two examples in the Appendix, in which a table indicates whether the identical sensor system can be optimal or not for n varying from 2 to 23. The table reveals that for some finite number of sensors, it is still possible that the simple identical sensor system performs optimally even if the simple identical sensor system performs suboptimally as n goes to infinity. Following their work, we will provide more situations that the simple identical sensor system is only suboptimal in this thesis. Details will be given in the subsequent chapters.

Chapter 2

Preliminaries

In this chapter, we define the notations we use in this thesis and present the background knowledge respectively in Sections 2.1 and 2.2. The system model follows exactly what has been adopted in [1].

2.1 System Model

In this thesis, we consider a parallel distributed detection system with ternary local observation from $\{a_1, a_2, a_3\}$ and binary local quantization. This should be the simplest model in the respective research domain. Through the study of such a simple system, we intend to give a preliminary answer to the general query that under which condition the so-called identical quantizer system is optimal in detection error.

In our setting, the two hypotheses are assumed equally likely. The statistics for local

observations in $\{a_1, a_2, a_3\}$ is denoted parametrically by:

$$\begin{aligned}
\Pr(a_1|H_0) &= P_1 \\
\Pr(a_2|H_0) &= P_2 \\
\Pr(a_3|H_0) &= 1 - P_1 - P_2 \\
\Pr(a_1|H_1) &= 1 - Q_1 - Q_2 \\
\Pr(a_2|H_1) &= Q_1 \\
\Pr(a_3|H_1) &= Q_2
\end{aligned}$$

They can be listed in a tabular form as follows.

y	a_1	a_2	a_3
$\Pr(y\|H_0)$	P_1	P_2	$1-P_1-P_2$
$\Pr(y\|H_1)$	$1-Q_1-Q_2$	Q_1	Q_2

Based on the above setting, there are only two nontrivial deterministic likelihood ratio quantizers (LRQs) if either

$$\frac{\Pr(a_1|H_1)}{\Pr(a_1|H_0)} \geq \frac{\Pr(a_2|H_1)}{\Pr(a_2|H_0)} \geq \frac{\Pr(a_3|H_1)}{\Pr(a_3|H_0)} \tag{2.1}$$

or

$$\frac{\Pr(a_1|H_1)}{\Pr(a_1|H_0)} \leq \frac{\Pr(a_2|H_1)}{\Pr(a_2|H_0)} \leq \frac{\Pr(a_3|H_1)}{\Pr(a_3|H_0)} \tag{2.2}$$

holds. These two LRQs are $\hat{g}$, which partitions local observation space $\{a_1, a_2, a_3\}$ to $\{a_1\}$ and $\{a_2, a_3\}$, and $\bar{g}$, which partitions local observation space $\{a_1, a_2, a_3\}$ to $\{a_1, a_2\}$ and $\{a_3\}$. For ordering relations of likelihood ratios other than (2.1) and (2.2), we can do similar partitions by re-indexing the local observations and hence they are included in the cases we discuss in the sequel. The resulting post-partition or post-quantization distributions for random quantizer output u respectively for $\hat{g}$ and $\bar{g}$ are illustrated in Table 2.1.

Because the local observations $Y_1, \ldots, Y_n$ are i.i.d., each local sensor in the optimal system should adopt either $\hat{g}$ or $\bar{g}$ as the local quantizer. Assume that m out of n local

Table 2.1:

u	0	1
$P_{\hat{g}}(u) = \Pr(u\|H_0)$	P_1	$1 - P_1$
$Q_{\hat{g}}(u) = \Pr(u\|H_1)$	$1-Q_1-Q_2$	$Q_1 + Q_2$
u	0	1
$P_{\bar{g}}(u) = \Pr(u\|H_0)$	$P_1 + P_2$	$1 - P_1 - P_2$
$Q_{\bar{g}}(u) = \Pr(u\|H_1)$	$1 - Q_2$	Q_2

quantizers used the quantization rule $\hat{g}$; then, the remaining $n - m$ sensors accommodate the quantization rule $\bar{g}$. By this assumption, the detection error is given by:

$$\begin{aligned} P_e(m,n) &= \frac{1}{2}\sum_{x=0}^{m}\sum_{y=0}^{n-m}\min\left\{\binom{m}{x}P_1^x(1-P_1)^{m-x}\binom{n-m}{y}(P_1+P_2)^y(1-P_1-P_2)^{n-m-y},\right. \\ &\qquad \left.\binom{m}{x}(1-Q_1-Q_2)^x(Q_1+Q_2)^{m-x}\binom{n-m}{y}(1-Q_2)^y Q_2^{n-m-y}\right\} \end{aligned}$$

where x and y are respectively the numbers of $\hat{g}$-sensors and $\bar{g}$-sensors that report 1 to the future center. In particular, when all the sensors assume quantization rule $\bar{g}$, which corresponds to $m = 0$, the detection error becomes:

$$P_e(0,n) = \frac{1}{2}\sum_{y=0}^{n}\min\left\{\binom{n}{y}(P_1+P_2)^y(1-P_1-P_2)^{n-y}, \binom{n}{y}(1-Q_2)^y Q_2^{n-y}\right\}$$

In contrast, if all sensors adopt quantization rule $\hat{g}$, implying $m = n$, the detection error is reduced to:

$$P_e(n,n) = \frac{1}{2}\sum_{x=0}^{n}\min\left\{\binom{n}{x}P_1^x(1-P_1)^{n-x}, \binom{n}{x}(1-Q_1-Q_2)^x(Q_1+Q_2)^{n-x}\right\}.$$

2.2 Background on Distributed Detection

The study of this thesis is basically a followup work to [1]. Some key results in [1] are therefore summarized in this subsection.

In the appendix, the authors in [1] demonstrated a counterexample that as the number of local quantizers n goes to infinity, the *identical quantizer system* is not optimal in detection. In that counterexample, binary hypotheses, ternary observation space $\{a_1, a_2, a_3\}$ and binary local quantization are assumed. The two hypothesis distributions are specified as indicated below.

Y	a_1	a_2	a_3
$P(y) = \Pr(y\|H_0)$	$\frac{1}{12}$	$\frac{1}{4}$	$\frac{2}{3}$
$Q(y) = \Pr(y\|H_1)$	$\frac{1}{3}$	$\frac{1}{3}$	$\frac{1}{3}$
$(dP/dQ)(y)$	$\frac{1}{4}$	$\frac{3}{4}$	2

Under this setting, there are only two nontrivial deterministic LRQ's, as having been stated in the previous subsection. Their post-quantization distributions are listed in Table 2.2.

Table 2.2:

u	0	1
$P_{\hat{g}}(u)$	$\frac{1}{12}$	$\frac{11}{12}$
$Q_{\hat{g}}(u)$	$\frac{1}{3}$	$\frac{2}{3}$

u	0	1
$P_{\bar{g}}(u)$	$\frac{1}{3}$	$\frac{2}{3}$
$Q_{\bar{g}}(u)$	$\frac{2}{3}$	$\frac{1}{3}$

Denote by $\gamma_n(\pi)$ as the Bayes detection error for a distributed system with $(n-1)$ $\bar{g}$-sensors and one g-sensor, where g could be either $\hat{g}$ or $\bar{g}$. Abbreviate $(u_1, ..., u_n)$ as u_1^n. Note that the best identical quantizer system should assume $\bar{g}$ for all sensors.

We then derive:

$$\begin{aligned}
\gamma_n\left(\frac{1}{2}\right) &= \frac{1}{2}\sum_{u_1^n\in\{0,1\}^n}\left[P_{\bar{g}}(u_1^{n-1})P_g(u_n)\wedge Q_{\bar{g}}(u_1^{n-1})Q_g(u_n)\right] \\
&= \frac{1}{2}\sum_{u_1^{n-1}\in\{0,1\}^{n-1}}\sum_{u_n\in\{0,1\}^n}\left[P_{\bar{g}}(u_1^{n-1})P_g(u_n)\wedge Q_{\bar{g}}(u_1^{n-1})Q_g(u_n)\right] \\
&= \sum_{u_1^{n-1}\in\{1,2\}^{n-1}}\left(\frac{P_{\bar{g}}(u_1^{n-1})+Q_{\bar{g}}(u_1^{n-1})}{2}\right)\gamma_1\left(\frac{P_{\bar{g}}(u_1^{n-1})}{P_{\bar{g}}(u_1^{n-1})+Q_{\bar{g}}(u_1^{n-1})}\right) \qquad (2.3)
\end{aligned}$$

where $\gamma_1(\cdot)$ is the Bayes detection error for a system with only one sensor, and we use for notational convenience $(x\wedge y)$ to denote $\min\{x,y\}$.

Taking the distribution in Table 2.2 into (2.3) and using l to indicate the number of 1's in u_1^{n-1}, we obtain

$$\gamma_n\left(\frac{1}{2}\right) = \sum_{l=0}^{n-1}\binom{n-1}{l}\left(\frac{2^l+2^{n-l-1}}{2\cdot 3^{n-1}}\right)\cdot\gamma_1\left(\frac{2^{2l-n+1}}{2^{2l-n+1}+1}\right). \qquad (2.4)$$

The last output u_n can be resulted from either local quantization rule $\hat{g}$ or $\bar{g}$. Accordingly, γ_1 can have two different formulas, which are respectively denoted by $\hat{\gamma}_1$ and $\bar{\gamma}_1$ for quantization rules $\hat{g}$ and $\bar{g}$. Their formulas are:

$$\hat{\gamma}_1(\pi) = \left(\frac{1}{12}\pi \ \wedge\ \frac{1}{3}(1-\pi)\right)+\left(\frac{11}{12}\pi \ \wedge\ \frac{2}{3}(1-\pi)\right)$$

and

$$\bar{\gamma}_1(\pi) = \left(\frac{1}{3}\pi \ \wedge\ \frac{2}{3}(1-\pi)\right)+\left(\frac{2}{3}\pi \ \wedge\ \frac{1}{3}(1-\pi)\right),$$

where their curves are plotted in Figure 2.1. Note that $\hat{\gamma}_1(\pi)=\bar{\gamma}_1(\pi)$ for $0\le\pi\le 1/3$, $\pi=4/7$ and $4/5\le\pi\le 1$. Thus the critical values of l in (2.4) are those for which $2^{2l-n+1}/(2^{2l-n+1}+1)$ lies in the union of $(1/3,4/7)$ and $(4/7,4/5)$. Equivalently, the critical l's lies in

$$\frac{n-2}{2}<l<\frac{n+1-\log_2(3)}{2}\approx\frac{n-0.585}{2} \quad \text{and} \quad \frac{n+1-\log_2(3)}{2}<l<\frac{n+1}{2}.$$

When $n = 2k$ is even,

$$k - 1 < l < \frac{2k + 1 - \log_2(3)}{2} \approx k - 0.292 \quad \text{and} \quad k - 0.292 < l < k + 0.5.$$

So the only critical value of l is $n/2 = k$, which implies that

$$\frac{2^{2l-n+1}}{2^{2l-n+1} + 1} = \frac{2}{3}.$$

Since $\hat{\gamma}(2/3) = 5/18 < 1/3 = \bar{\gamma}(2/3)$, there exists a *non-identical quantizer system* performed better than the best identical quantizer system. Hence, the optimal system must be a non-identical quantizer system.

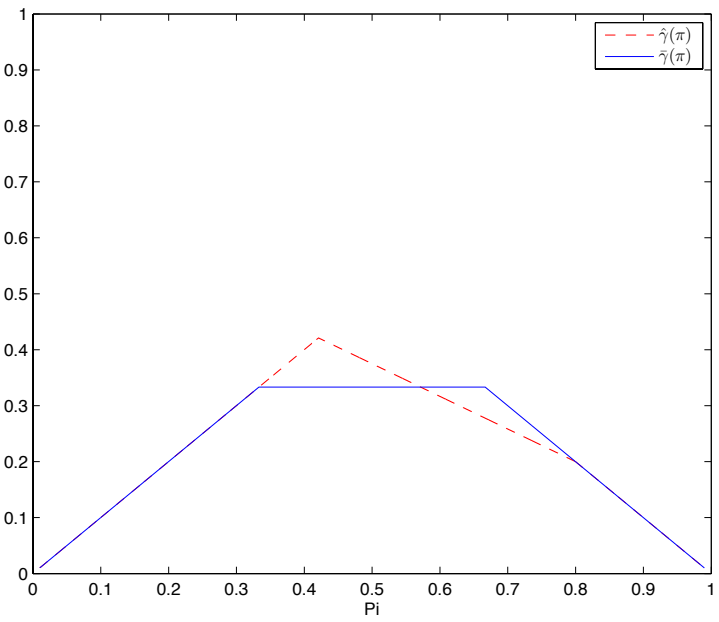

Figure 2.1: Functions of $\hat{\gamma}_1(\pi)$ and $\bar{\gamma}_1(\pi)$, where $\hat{\gamma}_1(\pi)$ is plotted in solid blue color, while $\bar{\gamma}_1(\pi)$ in dotted red color.

To be specific,

$$\begin{aligned} \gamma^*_{2k}\left(\frac{1}{2}\right) - \gamma^{\diamond}_{2k}\left(\frac{1}{2}\right) &\geq \binom{2k-1}{k}\left[\frac{2^k + 2^{k-1}}{2 \cdot 3^{2k-1}}\right]\left[\bar{\gamma}\left(\frac{2}{3}\right) - \hat{\gamma}\left(\frac{2}{3}\right)\right] \\ &= \frac{1}{8}\binom{2k-1}{k}\left(\frac{2}{9}\right)^k, \end{aligned} \tag{2.5}$$

where $\gamma_{2k}^{*}(1/2)$ and $\gamma_{2k}^{\diamond}(1/2)$ denote the detector errors for the optimal (surely, non-identical quantizer, in this counterexample) system and the best identical quantizer system, respectively. Based on (2.5), it can be proved that the ratio $\gamma_{2k}^{*}(\pi)/\gamma_{2k}^{\diamond}(\pi)$ will be strictly less than one as $k \to \infty$.

Chapter 3

Sufficient Conditions For Suboptimality Of Identical Quantizer System

In this chapter, we examine the optimality of the *identical quantizer system* (IQS) for various source statistics and determine under which condition the IQS is suboptimal.

In the previous chapter, we have provided an exemplified hypothesis distribution pair that the IQS is not optimal. However, in general, it is hard to known whether the IQS is suboptimal or not simply by the given hypothesis distribution pair unless detection errors of all possible designs (including the identical quantizer systems and non-identical quantizer systems) are exhausted. Nonetheless, in order to find the sufficient rule on hypothesis distributions, under which the IQS is suboptimal. We first resort to exhaustive numerical computations when the number of sensors is feasibly small, hoping to induce the possible rule from massive number of observations.

From the computations we have carried out, it seems that there does exist a certain line or area patterns of hypothesis distributsions such that the NQS (an acronym of non-identical quantizer system) is a better choice than the IQS.

Specifically, in Section 3.1, we will mention our preliminary works and some experiments

we have carried out. As there are only few publications devoting to this problem due to its intractability, we have to perform massive number of experiments to observe the possible trend for some specific cases. In Section 3.2, we will focus on those specific distributed detection systems, where the NQS performs strictly better than the IQS.

3.1 The Best Quantizers for Finite Number of Sensors

We now perform numerical experiments in this section so as to find the pattern for the sub optimality of the IQS.

For the ternary local observations, there are two nontrivial LRQs $\bar{g}$ and $\hat{g}$ as mentioned in the previous chapter. Our approach is to find the best IQS and then to replace one of the quantizers by a distinct one, which we will refer to it for convenience as the near-IQS in the sequel. If the latter has better detection error, then the optimal NQS (which performs surely better than the near-IQS) is apparently better than the best IQS.

Of course, when the number of sensors is small such as 20, we can test all possible combinations of quantizers and determine the true optimal design. In certain situations of the given hypothesis distributions, however, we do find that the IQS is always optimal for all the sensor number n we test. In other cases, whether the IQS is optimal depending on n. However, it is possible that the optimal NQS has two sensors using district quantizers instead of just one. Some optimal design even assumes three or four distinct quantizers. Thus, it is somewhat hard to identify the rule for the construction of the optimal NQS. This is perhaps the reason why only asymptotic results are available in this literature.

3.2 Finding the Particular Hypothesis Distributions That the IQS Is Better Than the Near-IQS

3.2.1 Case 1: Uniform Alternative Hypothesis Distribution

We first examine the specific case that the alternative hypothesis distribution is uniform. By this setting, only the null hypothesis distribution needs to be varied. The statistics for local observations $\{a_1, a_2, a_3\}$ can be given as follows.

$$\begin{aligned}\Pr(a_1|H_0) &= P_1\\ \Pr(a_2|H_0) &= P_2\\ \Pr(a_3|H_0) &= 1 - P_1 - P_2\end{aligned}$$

and

$$\begin{aligned}\Pr(a_1|H_1) &= \tfrac{1}{3}\\ \Pr(a_2|H_1) &= \tfrac{1}{3}\\ \Pr(a_3|H_1) &= \tfrac{1}{3}\end{aligned}$$

where P_1 and P_2 range from 0 to 1 under the restriction that $P_1 + P_2 < 1$. The above formula can be listed in a tabular form below.

y	a_1	a_2	a_3
$\Pr(y\|H_0)$	P_1	P_2	$1 - P_1 - P_2$
$\Pr(y\|H_1)$	$\frac{1}{3}$	$\frac{1}{3}$	$\frac{1}{3}$

Based on this table, there are three possible post-quantization LRQ's resulted, which are respectively classified as *type 1*, *type 2*, and *type 3* as shown in Table 3.1. We would like to stress again that among these three, there are only two nontrivial LRQ's after P_1 and P_2 are given.

We then increase P_1 and P_2 from 0 to 1 under $P_1 + P_2 < 1$. During this process, we fix the number of sensors n. Our experimental results indicate which IQS (among type-1 IQS,

Table 3.1: The condition on P_1 and P_2 specified below is the range in which the respective post-quantization LRQ is of effectively use in detection.

(a) $P_1 > \max\{P_2, (1-P_2)/2\}$ or $P_1 < \min\{P_2, (1-P_2)/2\}$

u	$0 \equiv \{a_1\}$	$1 \equiv \{a_2, a_3\}$
$P_{g_1}(u)$	P_1	$1-P_1$
$Q_{g_1}(u)$	$\frac{1}{3}$	$\frac{2}{3}$

(b) $\min\{P_2, 1-2P_2\} < P_1 < \max\{P_2, 1-2P_2\}$

u	$0 \equiv \{a_2\}$	$1 \equiv \{a_1, a_3\}$
$P_{g_2}(u)$	P_2	$1-P_2$
$Q_{g_2}(u)$	$\frac{1}{3}$	$\frac{2}{3}$

(c) $P_1 < \min\{(1-P_2)/2, 1-2P_2\}$ or $P_1 > \max\{(1-P_2)/2, 1-2P_2\}$

u	$0 \equiv \{a_1, a_2\}$	$1 \equiv \{a_3\}$
$P_{g_3}(u)$	P_1+P_2	$1-P_1-P_2$
$Q_{g_3}(u)$	$\frac{2}{3}$	$\frac{1}{3}$

type-2 IQS, and type-3 IQS) should be used can be clearly characterized into six regions. It would then be of interest, if we could identify the formulas of the six boundaries.

By denoting the error probabilities of the IQS for type 1, type 2 and type 3 local quantizers respectively by $\gamma_{n,1}$, $\gamma_{n,2}$ and $\gamma_{n,3}$, we derive for different P_1 and P_2 as follows:

$$\begin{aligned}
\gamma_{n,1}\left(\frac{1}{2}\right) &= \sum_{l=0}^{n-1}\binom{n-1}{l}\left(\frac{P_1^l(1-P_1)^{n-1-l}+(\frac{1}{3})^l(\frac{2}{3})^{n-1-l}}{2}\right)\gamma_{1,1}\left(\frac{P_1^l(1-P_1)^{n-1-l}}{P_1^l(1-P_1)^{n-1-l}+(\frac{1}{3})^l(\frac{2}{3})^{n-1-l}}\right) \\
&= \sum_{l=0}^{n-1}\binom{n-1}{l}\left(\frac{P_1^l(1-P_1)^{n-1-l}}{2\pi}\right)\left\{\left[P_1\pi \wedge \frac{1}{3}(1-\pi)\right]+\left[(1-P_1)\pi \wedge \frac{2}{3}(1-\pi)\right]\right\} \\
&= \frac{1}{2}\sum_{l=0}^{n-1}\binom{n-1}{l}\left\{\left[P_1^{l+1}(1-P_1)^{n-1-l} \wedge (\frac{1}{3})^{l+1}(\frac{2}{3})^{n-1-l}\right]+\left[P_1^l(1-P_1)^{n-l} \wedge (\frac{1}{3})^l(\frac{2}{3})^{n-l}\right]\right\}
\end{aligned} \tag{3.1}$$

$$\gamma_{n,2}\left(\frac{1}{2}\right) = \frac{1}{2}\sum_{l=0}^{n-1}\binom{n-1}{l}\left\{\left[P_2^{l+1}(1-P_2)^{n-1-l} \wedge (\frac{1}{3})^{l+1}(\frac{2}{3})^{n-1-l}\right] + \left[P_2^{l}(1-P_2)^{n-l} \wedge (\frac{1}{3})^{l}(\frac{2}{3})^{n-l}\right]\right\} \tag{3.2}$$

$$\gamma_{n,3}\left(\frac{1}{2}\right) = \frac{1}{2}\sum_{l=0}^{n-1}\binom{n-1}{l}\left\{\left[P_3^{l+1}(1-P_3)^{n-1-l} \wedge (\frac{2}{3})^{l+1}(\frac{1}{3})^{n-1-l}\right] + \left[P_3^{l}(1-P_3)^{n-l} \wedge (\frac{2}{3})^{l}(\frac{1}{3})^{n-l}\right]\right\} \tag{3.3}$$

where for convenience, we let $P_3 = 1 - P_1 - P_2$. With the availability of these error formulas, the boundaries of the six regions can be characterized by the following six formulas:

$$\begin{aligned}
&\gamma_{n,1}\left(\tfrac{1}{2}\right) = \gamma_{n,2}\left(\tfrac{1}{2}\right) \text{ for } 0 < P_1 < \tfrac{1}{3} \text{ and } \tfrac{1}{3} < P_2 < 1\\
&\gamma_{n,1}\left(\tfrac{1}{2}\right) = \gamma_{n,2}\left(\tfrac{1}{2}\right) \text{ for } \tfrac{1}{3} < P_1 < 1 \text{ and } 0 < P_2 < \tfrac{1}{3}\\
&\gamma_{n,1}\left(\tfrac{1}{2}\right) = \gamma_{n,3}\left(\tfrac{1}{2}\right) \text{ for } \tfrac{1}{3} < P_1 < 1 \text{ and } 0 < P_2 < \tfrac{1}{3}\\
&\gamma_{n,1}\left(\tfrac{1}{2}\right) = \gamma_{n,3}\left(\tfrac{1}{2}\right) \text{ for } 0 < P_1 < \tfrac{1}{3} \text{ and } 0 < P_2 < \tfrac{1}{3}\\
&\gamma_{n,2}\left(\tfrac{1}{2}\right) = \gamma_{n,3}\left(\tfrac{1}{2}\right) \text{ for } 0 < P_1 < \tfrac{1}{3} \text{ and } 0 < P_2 < \tfrac{1}{3}\\
&\gamma_{n,2}\left(\tfrac{1}{2}\right) = \gamma_{n,3}\left(\tfrac{1}{2}\right) \text{ for } 0 < P_1 < \tfrac{1}{3} \text{ and } \tfrac{1}{3} < P_2 < 1
\end{aligned}$$

They are respectively drawn in Figure 3.1.

In (3.1), (3.2), and (3.3), "$\wedge$" means to take the smaller value of the two quantities across it. So these formulas can be transformed to other shapes if the thresholds, beyond or under which the smaller one between the two quantities can be identified, are known.

Take (3.1) and (3.2) as examples. Let the thresholds l_{11}, l_{12}, l_{21}, and l_{22} be defined according to the below relations:

$$\begin{aligned}
&P_1^{l+1}(1-P_1)^{n-1-l} > (\tfrac{1}{3})^{l+1}(\tfrac{2}{3})^{n-1-l} && \text{for } l < l_{11}\\
&P_1^{l}(1-P_1)^{n-l} > (\tfrac{1}{3})^{l}(\tfrac{2}{3})^{n-l} && \text{for } l < l_{12}\\
&P_2^{l+1}(1-P_2)^{n-1-l} > (\tfrac{1}{3})^{l+1}(\tfrac{2}{3})^{n-1-l} && \text{for } l < l_{21}\\
&P_2^{l}(1-P_2)^{n-l} > (\tfrac{1}{3})^{l}(\tfrac{2}{3})^{n-l} && \text{for } l < l_{22}
\end{aligned}$$

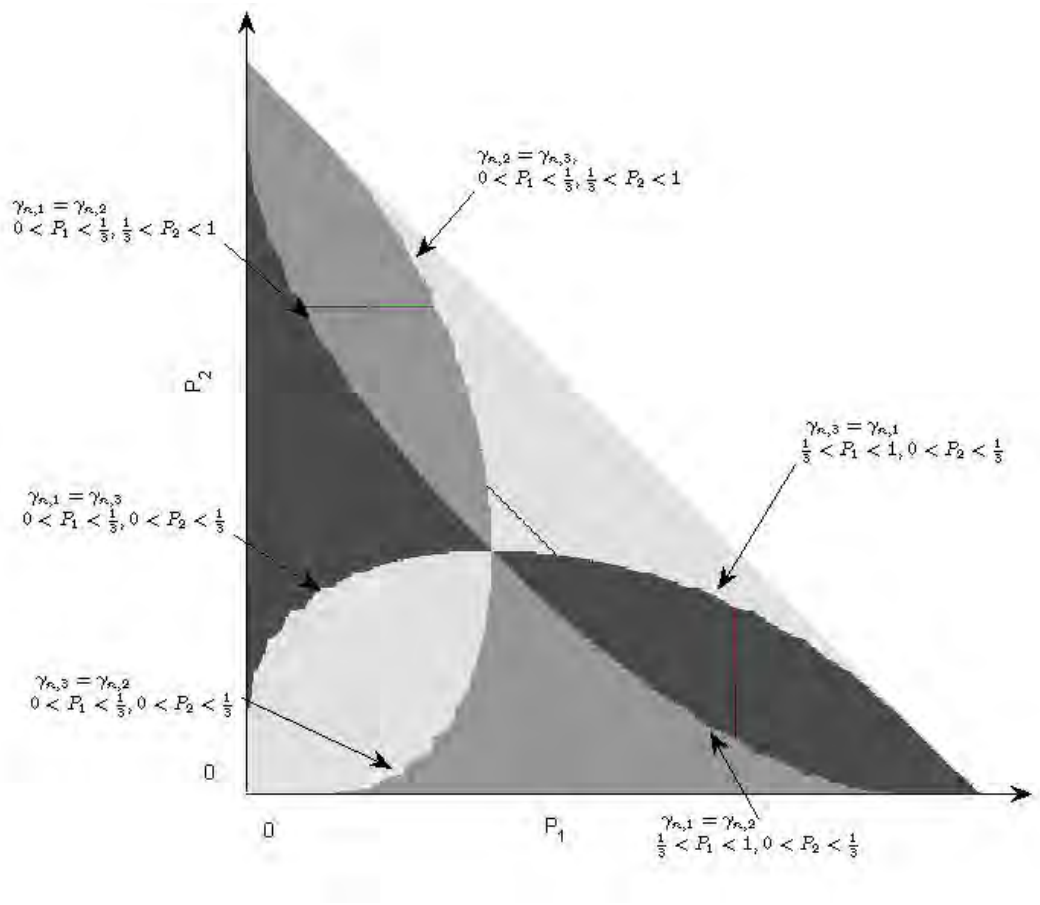

Figure 3.1: Regions of the best IQSs. The dark-gray, gray and light-gray areas respectively correspond to the regions that $\gamma_{n,1}$, $\gamma_{n,2}$, and $\gamma_{n,3}$ are the best IQSs. In addition, the line sections of colors dark red, light red, dark green, light green, dark blue and light blue correspond to Segments 1, 2, 3, 4, 5 and 6, respectively, described in (3.5).

Bases on these thresholds, we can re-write (3.1) and (3.2) as follows.

$$\begin{aligned}
\gamma_{n,1}\left(\frac{1}{2}\right) &= \frac{1}{2}\sum_{l=0}^{l_{11}-1}\binom{n-1}{l}\left[(\frac{1}{3})^{l+1}(\frac{2}{3})^{n-1-l}+(\frac{1}{3})^{l}(\frac{2}{3})^{n-l}\right] \\
&+ \frac{1}{2}\sum_{l=l_{11}}^{l_{12}-1}\binom{n-1}{l}\left[P_1^{l+1}(1-P_1)^{n-1-l}+(\frac{1}{3})^{l}(\frac{2}{3})^{n-l}\right] \\
&+ \frac{1}{2}\sum_{l=l_{12}}^{n-1}\binom{n-1}{l}\left[P_1^{l+1}(1-P_1)^{n-1-l}+P_1^{l}(1-P_1)^{n-l}\right]
\end{aligned}$$

$$\begin{aligned}\gamma_{n,2}\left(\frac{1}{2}\right) &= \frac{1}{2}\sum_{l=0}^{l_{21}-1}\binom{n-1}{l}\left[(\frac{1}{3})^{l+1}(\frac{2}{3})^{n-1-l}+(\frac{1}{3})^{l}(\frac{2}{3})^{n-l}\right] \\ &+ \frac{1}{2}\sum_{l=l_{21}}^{l_{22}-1}\binom{n-1}{l}\left[P_2^{l+1}(1-P_2)^{n-1-l}+(\frac{1}{3})^{l}(\frac{2}{3})^{n-l}\right] \\ &+ \frac{1}{2}\sum_{l=l_{22}}^{n-1}\binom{n-1}{l}\left[P_2^{l+1}(1-P_2)^{n-1-l}+P_2^{l}(1-P_2)^{n-l}\right].\end{aligned}$$

Examining

$$\gamma_{n,1}\left(\frac{1}{2}\right)=\gamma_{n,2}\left(\frac{1}{2}\right), \tag{3.4}$$

we can rewrite it as

$$\begin{aligned}&\frac{1}{2}\sum_{l=|l_{11}-l_{21}|+1}^{\max\{l_{11}-1,l_{21}-1\}}\binom{n-1}{l}\left[(\frac{1}{3})^{l+1}(\frac{2}{3})^{n-1-l}+(\frac{1}{3})^{l}(\frac{2}{3})^{n-l}\right]+\frac{1}{2}\sum_{l=\min\{l_{11},l_{21}\}}^{\max\{l_{11},l_{21}\}-1}\binom{n-1}{l}\left[(\frac{1}{3})^{l}(\frac{2}{3})^{n-l}\right] \\ &+\frac{1}{2}\sum_{l=l_{12}}^{n-1}\binom{n-1}{l}\left[P_1^{l+1}(1-P_1)^{n-1-l}+P_1^{l}(1-P_1)^{n-l}\right]+\frac{1}{2}\sum_{l=l_{11}}^{l_{12}-1}\binom{n-1}{l}\left[P_1^{l+1}(1-P_1)^{n-1-l}\right] \\ &-\frac{1}{2}\sum_{l=l_{11}}^{l_{12}-1}\binom{n-1}{l}\left[P_2^{l+1}(1-P_2)^{n-1-l}\right]+\frac{1}{2}\sum_{l=\min\{l_{22},l_{12}\}+1}^{\max\{l_{12},l_{22}\}}\binom{n-1}{l}\left[(\frac{1}{3})^{l}(\frac{2}{3})^{n-l}\right] \\ &-\frac{1}{2}\sum_{l=l_{22}}^{n-1}\binom{n-1}{l}\left[P_2^{l+1}(1-P_2)^{n-1-l}+P_2^{l}(1-P_2)^{n-l}\right]=0.\end{aligned}$$

As a result, the boundary formula becomes a function of four parameters l_{11}, l_{12}, l_{21}, and l_{22}, each of which ranges from 0 to n. By this, we can plot the boundaries of the six regions directly. Nevertheless, further simplification of the boundary formulas might require specific conditions on the hypothesis distributions, and is deferred as the future work.

3.2.2 Regions that the IQS is Suboptimal

After identifying the best IQS for a given hypothesis distribution, we next test whether the NQS can improve the best IQS or not. As aforementioned, it would be easier to disprove the optimality of the IQS rather than proving its optimality because we only need to show the existence of an NQS that outperforms the best IQS.

To achieve this goal, we choose to replace one of the sensors' LRQ by a distinct one. By this, we may possibly identify some area on the hypothesis distribution domain, which the NQS outperforms the IQS. However, we found that such areas may be changed for different number of sensors n. We then ask ourselves whether there exists a specific area that the NQS is always better than the IQS for most n. For this purpose, we overlap our experimental results for different n and look for the common area that the NQS (or more specifically, the near-IQS) is better. We found some desired common areas:

$$\begin{aligned}
&\text{Segment 1: } (n-1) \text{ type } 1 + 1 \text{ type } 2 : P_1 = \tfrac{2}{3}, \tfrac{5}{64} \le P_2 < \tfrac{1}{6} \\
&\text{Segment 2: } (n-1) \text{ type } 1 + 1 \text{ type } 3 : P_1 = \tfrac{2}{3}, \tfrac{1}{6} < P_2 \le \tfrac{49}{192} \\
&\text{Segment 3: } (n-1) \text{ type } 2 + 1 \text{ type } 1 : P_2 = \tfrac{2}{3}, \tfrac{5}{64} \le P_1 < \tfrac{1}{6} \\
&\text{Segment 4: } (n-1) \text{ type } 2 + 1 \text{ type } 3 : P_2 = \tfrac{2}{3}, \tfrac{1}{6} < P_1 \le \tfrac{49}{192} \\
&\text{Segment 5: } (n-1) \text{ type } 3 + 1 \text{ type } 1 : P_1 + P_2 = \tfrac{3}{4}, \tfrac{21}{64} \le P_1 < \tfrac{3}{8}, \tfrac{3}{8} < P_2 \le \tfrac{27}{64} \\
&\text{Segment 6: } (n-1) \text{ type } 3 + 1 \text{ type } 2 : P_1 + P_2 = \tfrac{3}{4}, \tfrac{3}{8} < P_1 \le \tfrac{27}{64}, \tfrac{21}{64} \le P_2 < \tfrac{3}{8}
\end{aligned} \tag{3.5}$$

Now take the first segment as an example. We have already known that the type-1 IQS is the best IQS in the specified ranges of P_1 and P_2. We then replace one of the local quantizer to a type-2 quantizer $\hat{g}$. For reader's convenience, the post-quantization hypothesis distributions of the type-1 and type-2 quantizers are tabulated in Table 3.2.

Table 3.2:

u	0	1
$P_{\bar{g}}(u)$	P_1	$1 - P_1$
$P_{\bar{g}}(u)$	$\frac{1}{3}$	$\frac{2}{3}$

u	0	1
$P_{\hat{g}}(u)$	P_2	$1 - P_2$
$Q_{\hat{g}}(u)$	$\frac{1}{3}$	$\frac{2}{3}$

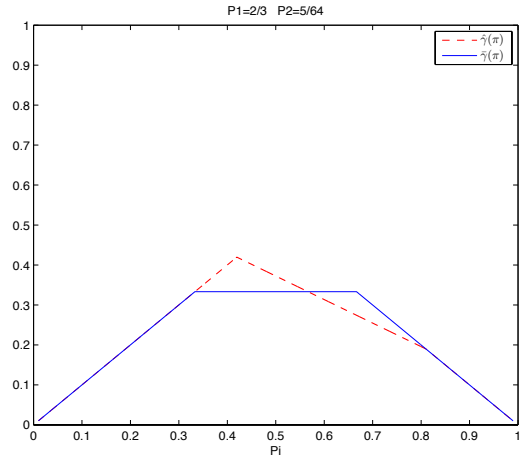

(a) $P_1 = \frac{2}{3}$ and $P_2 = \frac{5}{64}$

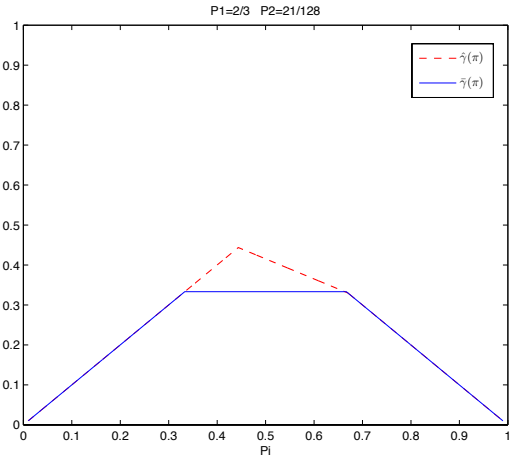

(b) $P_1 = \frac{2}{3}$ and $P_2 = \frac{21}{128}$

Figure 3.2: Functions of $\hat{\gamma}_1(\pi)$ and $\bar{\gamma}_1(\pi)$, where $\hat{\gamma}_1(\pi)$ is plotted in solid blue color, while $\bar{\gamma}_1(\pi)$ in dotted red color.

Using the same technique introduced in Chapter 2, we derive:

$$\begin{aligned}
\gamma_n\left(\frac{1}{2}\right) &= \frac{1}{2}\sum_{u_1^n\in\{0,1\}^n}\left[P_{\bar{g}}(u_1^{n-1})P_g(u_n)\wedge Q_{\bar{g}}(u_1^{n-1})Q_g(u_n)\right] \\
&= \frac{1}{2}\sum_{u_1^{n-1}\in\{0,1\}^{n-1}}\sum_{u_n\in\{0,1\}^n}\left[P_{\bar{g}}(u_1^{n-1})P_g(u_n)\wedge Q_{\bar{g}}(u_1^{n-1})Q_g(u_n)\right] \\
&= \sum_{u_1^{n-1}\in\{1,2\}^{n-1}}\left(\frac{P_{\bar{g}}(u_1^{n-1})+Q_{\bar{g}}(u_1^{n-1})}{2}\right)\gamma_1\left(\frac{P_{\bar{g}}(u_1^{n-1})}{P_{\bar{g}}(u_1^{n-1})+Q_{\bar{g}}(u_1^{n-1})}\right). \quad (3.6)
\end{aligned}$$

Taking the distributions in Table 3.2 into (3.6), we can rewrite (3.6) as

$$\gamma_n\left(\frac{1}{2}\right)=\sum_{l=0}^{n-1}\binom{n-1}{l}\left(\frac{P_1^l(1-P_1)^{n-1-l}+(\frac{1}{3})^l(\frac{2}{3})^{n-1-l}}{2}\right)\gamma_1\left(\frac{1}{1+(\frac{1}{3P_1})^l(\frac{2}{3-3P_1})^{n-1-l}}\right) \quad (3.7)$$

By checking Fig. 3.2(a) under $P_1 = \frac{2}{3}$ and $P_2 = \frac{5}{64}$, the range that $\hat{\gamma}(\pi) \neq \bar{\gamma}(\pi)$ is the union of $(1/3, 64/113)$ and $(64/113, 64/79)$. So the critical l lies in

$$\frac{1}{3} < \frac{1}{1+2^{n-1-2l}} < \frac{64}{113} \quad \text{and} \quad \frac{64}{113} < \frac{1}{1+2^{n-1-2l}} < \frac{64}{79},$$

or equivalently,

$$\frac{n}{2} - 1 < l < \frac{n+5-2\log_2(7)}{2} \approx \frac{n}{2} - 0.307 \quad (3.8)$$

and

$$\frac{n+5-2\log_2(7)}{2} < l < \frac{n+5-\log_2(15)}{2} \approx \frac{n}{2} + 0.547. \tag{3.9}$$

Again, when $n = 2k$, it is not possible to have an integer l satisfying (3.8) but $l = n/2 = k$ makes valid (3.9).

Similar derivation can be applied to Fig. 3.2(b). The two ranges for Fig. 3.2(b) are $(1/3, 128/193)$ and $(128/193, 128/191)$, where $\hat{\gamma}(\pi)$ is larger than $\bar{\gamma}(\pi)$ in the former range but is smaller than $\bar{\gamma}(\pi)$ in the latter range. This results in the derivation that

$$\frac{1}{3} < \frac{1}{1+2^{n-1-2l}} < \frac{128}{193} \quad \text{and} \quad \frac{128}{193} < \frac{1}{1+2^{n-1-2l}} < \frac{128}{191},$$

or equivalently,

$$\frac{n}{2} - 1 < l < \frac{n}{2} + 3 - \frac{1}{2}\log_2(65) \approx \frac{n}{2} - 0.011 \tag{3.10}$$

and

$$\frac{n+5-2\log_2(7)}{2} < l < \frac{n}{2} + 3 - \frac{1}{2}\log_2(63) \approx \frac{n}{2} + 0.011. \tag{3.11}$$

Again, when $n = 2k$, it is not possible to have an integer l satisfying (3.10) but $l = n/2 = k$ makes valid (3.11).

A) Line Segment 1

We now give a general result for line segment 1. For $P_1 = 2/3$, the two gamma functions are given by:

$$\begin{aligned}
\bar{r}(\pi) &= \left[P_1\pi \ \wedge \ \frac{1}{3}(1-\pi)\right] + \left[(1-P_1)\pi \ \wedge \ \frac{2}{3}(1-\pi)\right] \\
&= \left[\frac{2}{3}\pi \ \wedge \ \frac{1}{3}(1-\pi)\right] + \left[\frac{1}{3}\pi \ \wedge \ \frac{2}{3}(1-\pi)\right] \\
&= \begin{cases} \frac{2}{3}\pi + \frac{1}{3}\pi, & 0 \le \pi < \frac{1}{3} \\ \frac{1}{3}(1-\pi) + \frac{1}{3}\pi, & \frac{1}{3} \le \pi < \frac{2}{3} \\ \frac{1}{3}(1-\pi) + \frac{2}{3}(1-\pi), & \frac{2}{3} \le \pi \le 1 \end{cases} \\
&= \begin{cases} \pi, & 0 \le \pi < \frac{1}{3} \\ \frac{1}{3}, & \frac{1}{3} \le \pi < \frac{2}{3} \\ 1-\pi, & \frac{2}{3} \le \pi \le 1 \end{cases}
\end{aligned}$$

and for $P_2 < 1 - P_1 = 1/3$,

$$\begin{aligned}
\hat{r}(\pi) &= \left[P_2\pi \ \wedge \ \frac{1}{3}(1-\pi)\right] + \left[(1-P_2)\pi \ \wedge \ \frac{2}{3}(1-\pi)\right] \\
&= \begin{cases} P_2\pi + (1-P_2)\pi, & 0 \le \pi < \frac{2}{5-3P_2} \\ P_2\pi + \frac{2}{3}(1-\pi), & \frac{2}{5-3P_2} \le \pi < \frac{1}{3P_2+1} \\ \frac{1}{3}(1-\pi) + \frac{2}{3}(1-\pi), & \frac{1}{3P_2+1} \le \pi \le 1 \end{cases} \\
&= \begin{cases} \pi, & 0 \le \pi < \frac{2}{5-3P_2} \\ P_2\pi + \frac{2}{3}(1-\pi), & \frac{2}{5-3P_2} \le \pi < \frac{1}{3P_2+1} \\ 1-\pi, & \frac{1}{3P_2+1} \le \pi \le 1 \end{cases}
\end{aligned}$$

The two ranges that $\hat{\gamma}(\pi) \neq \bar{\gamma}(\pi)$ are $(\frac{1}{3}, \frac{1}{2-3P_2})$ and $(\frac{1}{2-3P_2}, \frac{1}{3P_2+1})$, where $\hat{\gamma}(\pi)$ is larger than $\bar{\gamma}(\pi)$ in the former range but is smaller than $\bar{\gamma}(\pi)$ in the latter range. This results in the derivation that

$$\frac{1}{3} < \frac{1}{1+2^{n-1-2l}} < \frac{1}{2-3P_2} \quad \text{and} \quad \frac{1}{2-3P_2} < \frac{1}{1+2^{n-1-2l}} < \frac{1}{3P_2+1},$$

or equivalently,

$$\frac{n}{2} - 1 < l < \frac{n}{2} - \frac{1}{2} - \frac{1}{2}\log_2(1-3P_2) \tag{3.12}$$

and

$$\frac{n}{2} - \frac{1}{2} - \frac{1}{2}\log_2(1-3P_2) < l < \frac{n}{2} - \frac{1}{2} - \frac{1}{2}\log_2(3P_2). \tag{3.13}$$

Suppose $n = 2k$ is even. Therefore, if

$$k - \frac{1}{2} - \frac{1}{2}\log_2(1-3P_2) < k \quad (\text{i.e., } P_2 < \frac{1}{6}),$$

then no integer l satisfies (3.12). Note that $P_2 < \frac{1}{6}$ implies that $-\frac{1}{2} - \frac{1}{2}\log_2(1-3P_2) < 0$, and $-\frac{1}{2} - \frac{1}{2}\log_2(3P_2) > 0$. Hence, taking γ_1 to be $\hat{\gamma}$ in (3.7) always yields a smaller $\gamma_n(1/2)$. We conclude that when $P_1 = \frac{2}{3}$ and $0 \le P_2 < \frac{1}{6}$, using $(n-1)$ type 1 + 1 type 2 quantizers always outperform $\gamma_{n,1}$. Since Figure 3.1 indicates that $\gamma_{n,1}$ is the optimal IQS between the two margins of $\gamma_{n,1} = \gamma_{n,2}$ and $\gamma_{n,1} = \gamma_{n,3}$ for $\frac{1}{3} \le P_1 \le 1$ and $0 \le P_2 \le \frac{1}{3}$, we can then decide numerically that for the line segment decided by $P_1 = \frac{2}{3}$ and $\frac{5}{64} \le P_2 < \frac{1}{6}$, the IQS is only suboptimal.

Note that when $P_2 = \frac{1}{6}$, no integer satisfies both (3.12) and (3.13); hence, using $(n-1)$ type 1 + 1 type 2 quantizers have the same performance as $\gamma_{n,1}$. In such case, we can no longer claim that the IQS is only suboptimal.

B) Line Segment 2

We can similarly examine our result regarding line segment 2.

Again, for $P_1 = 2/3$, the two gamma functions are given by:

$$\begin{aligned}
\bar{r}(\pi) &= \left[P_1\pi \ \wedge \ \frac{1}{3}(1-\pi)\right] + \left[(1-P_1)\pi \ \wedge \ \frac{2}{3}(1-\pi)\right] \\
&= \left[\frac{2}{3}\pi \ \wedge \ \frac{1}{3}(1-\pi)\right] + \left[\frac{1}{3}\pi \ \wedge \ \frac{2}{3}(1-\pi)\right] \\
&= \begin{cases} \frac{2}{3}\pi + \frac{1}{3}\pi, & 0 \le \pi < \frac{1}{3} \\ \frac{1}{3}(1-\pi) + \frac{1}{3}\pi, & \frac{1}{3} \le \pi < \frac{2}{3} \\ \frac{1}{3}(1-\pi) + \frac{2}{3}(1-\pi), & \frac{2}{3} \le \pi \le 1 \end{cases} \\
&= \begin{cases} \pi, & 0 \le \pi < \frac{1}{3} \\ \frac{1}{3}, & \frac{1}{3} \le \pi < \frac{2}{3} \\ 1-\pi, & \frac{2}{3} \le \pi \le 1 \end{cases}
\end{aligned}$$

and denoting conveniently $P_{12} = P_1 + P_2 = \frac{2}{3} + P_2 \ge \frac{2}{3}$,

$$\hat{r}(\pi) = \left[P_{12}\pi \ \wedge \ \frac{2}{3}(1-\pi)\right] + \left[(1-P_{12})\pi \ \wedge \ \frac{1}{3}(1-\pi)\right].$$

It can be verified that $\frac{2}{3P_{12}+2} < \frac{1}{4-3P_{12}}$; hence,

$$\begin{aligned}
\hat{r}(\pi) &= \left[P_{12}\pi \ \wedge \ \frac{2}{3}(1-\pi)\right] + \left[(1-P_{12})\pi \ \wedge \ \frac{1}{3}(1-\pi)\right] \\
&= \begin{cases} P_{12}\pi + (1-P_{12})\pi, & 0 \le \pi < \frac{2}{3P_{12}+2} \\ \frac{2}{3}(1-\pi) + (1-P_{12})\pi, & \frac{2}{3P_{12}+2} \le \pi < \frac{1}{4-3P_{12}} \\ \frac{2}{3}(1-\pi) + \frac{1}{3}(1-\pi), & \frac{1}{4-3P_{12}} \le \pi \le 1 \end{cases} \\
&= \begin{cases} \pi, & 0 \le \pi < \frac{2}{3P_{12}+2} \\ \frac{2}{3} + \left(\frac{1}{3} - P_{12}\right)\pi, & \frac{2}{3P_{12}+2} \le \pi < \frac{1}{4-3P_{12}} \\ 1-\pi, & \frac{1}{4-3P_{12}} \le \pi \le 1 \end{cases}
\end{aligned}$$

The two ranges that $\hat{\gamma}(\pi) \neq \bar{\gamma}(\pi)$ are $(\frac{1}{3}, \frac{1}{3P_3-1})$ and $(\frac{1}{3P_3-1}, \frac{1}{4-3P_3})$, where $\hat{\gamma}(\pi)$ is larger than $\bar{\gamma}(\pi)$ in the former range but is smaller than $\bar{\gamma}(\pi)$ in the latter range. This results in the

derivation that

$$\frac{1}{3} < \frac{1}{1+2^{n-1-2l}} < \frac{1}{3P_{12}-1} \quad \text{and} \quad \frac{1}{3P_{12}-1} < \frac{1}{1+2^{n-1-2l}} < \frac{1}{4-3P_{12}},$$

or equivalently,

$$\frac{n}{2} - 1 < l < \frac{n}{2} - \frac{1}{2} - \frac{1}{2}\log_2(3P_{12}-2) \tag{3.14}$$

and

$$\frac{n}{2} - \frac{1}{2} - \frac{1}{2}\log_2(3P_{12}-2) < l < \frac{n}{2} - \frac{1}{2} - \frac{1}{2}\log_2(3-3P_{12}). \tag{3.15}$$

Suppose $n = 2k$ is even. Therefore, if

$$k - \frac{1}{2} - \frac{1}{2}\log_2(3P_{12}-2) < k \quad \left(\text{i.e., } P_{12} > \frac{5}{6}, \text{ or equivalently } P_2 > \frac{1}{6}\right),$$

then no integer l satisfies (3.14). Note that $P_{12} > \frac{5}{6}$ implies that $-\frac{1}{2} - \frac{1}{2}\log_2(3P_{12}-2) < 0$, and $-\frac{1}{2} - \frac{1}{2}\log_2(3-3P_{12}) > 0$. Hence, taking γ_1 to be $\hat{\gamma}$ in (3.7) always yields a smaller $\gamma_n(1/2)$. We conclude that when $P_1 = \frac{2}{3}$ and $\frac{1}{6} < P_2 \leq 1$, using $(n-1)$ type 1 + 1 type 3 quantizers always outperform $\gamma_{n,1}$. Since Figure 3.1 indicates that $\gamma_{n,1}$ is the optimal IQS between the two margins of $\gamma_{n,1} = \gamma_{n,2}$ and $\gamma_{n,1} = \gamma_{n,3}$ for $\frac{1}{3} \leq P_1 \leq 1$ and $0 \leq P_2 \leq \frac{1}{3}$, we can then decide numerically that for the line segment decided by $P_1 = \frac{2}{3}$ and $\frac{1}{6} < P_2 < \frac{49}{192}$, the IQS is only suboptimal.

Note that when $P_2 = \frac{1}{6}$, no integer satisfies both (3.14) and (3.15); hence, using $(n-1)$ type 1 + 1 type 3 quantizers have the same performance as $\gamma_{n,1}$. In such case, we can no longer claim that the IQS is only suboptimal.

C) Line Segment 3

We now prove the validity of line segment 3. For $P_2 = 2/3$, the two gamma functions are

given by:

$$\begin{aligned}
\bar{r}(\pi) &= \left[P_2\pi \ \wedge \ \frac{1}{3}(1-\pi)\right] + \left[(1-P_2)\pi \ \wedge \ \frac{2}{3}(1-\pi)\right] \\
&= \left[\frac{2}{3}\pi \ \wedge \ \frac{1}{3}(1-\pi)\right] + \left[\frac{1}{3}\pi \ \wedge \ \frac{2}{3}(1-\pi)\right] \\
&= \begin{cases} \frac{2}{3}\pi + \frac{1}{3}\pi, & 0 \le \pi < \frac{1}{3} \\ \frac{1}{3}(1-\pi) + \frac{1}{3}\pi, & \frac{1}{3} \le \pi < \frac{2}{3} \\ \frac{1}{3}(1-\pi) + \frac{2}{3}(1-\pi), & \frac{2}{3} \le \pi \le 1 \end{cases} \\
&= \begin{cases} \pi, & 0 \le \pi < \frac{1}{3} \\ \frac{1}{3}, & \frac{1}{3} \le \pi < \frac{2}{3} \\ 1-\pi, & \frac{2}{3} \le \pi \le 1 \end{cases}
\end{aligned}$$

and for $P_1 < 1 - P_2 = 1/3$,

$$\begin{aligned}
\hat{r}(\pi) &= \left[P_1\pi \ \wedge \ \frac{1}{3}(1-\pi)\right] + \left[(1-P_1)\pi \ \wedge \ \frac{2}{3}(1-\pi)\right] \\
&= \begin{cases} P_1\pi + (1-P_1)\pi, & 0 \le \pi < \frac{2}{3P_3+2} \\ P_1\pi + \frac{2}{3}(1-\pi), & \frac{2}{5-3P_1} \le \pi < \frac{1}{3P_1+1} \\ \frac{1}{3}(1-\pi) + \frac{2}{3}(1-\pi), & \frac{1}{3P_1+1} \le \pi \le 1 \end{cases} \\
&= \begin{cases} \pi, & 0 \le \pi < \frac{2}{3P_3+2} \\ \frac{2}{3} + \left(\frac{1}{3} - P_1\right)\pi, & \frac{2}{3P_3+2} \le \pi < \frac{1}{4-3P_3} \\ 1-\pi, & \frac{1}{4-3P_3} \le \pi \le 1 \end{cases}
\end{aligned}$$

The two ranges that $\hat{\gamma}(\pi) \neq \bar{\gamma}(\pi)$ are $(\frac{1}{3}, \frac{1}{2-3P_1})$ and $(\frac{1}{2-3P_1}, \frac{1}{3P_1+1})$, where $\hat{\gamma}(\pi)$ is larger than $\bar{\gamma}(\pi)$ in the former range but is smaller than $\bar{\gamma}(\pi)$ in the latter range. This results in the derivation that

$$\frac{1}{3} < \frac{1}{1+2^{n-1-2l}} < \frac{1}{2-3P_1} \quad \text{and} \quad \frac{1}{2-3P_1} < \frac{1}{1+2^{n-1-2l}} < \frac{1}{3P_1+1},$$

or equivalently,

$$\frac{n}{2} - 1 < l < \frac{n}{2} - \frac{1}{2} - \frac{1}{2}\log_2(1-3P_1) \tag{3.16}$$

and

$$\frac{n}{2} - \frac{1}{2} - \frac{1}{2}\log_2(1-3P_1) < l < \frac{n}{2} - \frac{1}{2} - \frac{1}{2}\log_2(3P_1). \tag{3.17}$$

Suppose $n = 2k$ is even. Therefore, if

$$k - \frac{1}{2} - \frac{1}{2}\log_2(1-3P_1) < k \quad \text{(i.e., } P_1 < \frac{1}{6}\text{)},$$

then no integer l satisfies (3.16). Note that $P_1 < \frac{1}{6}$ implies that $-\frac{1}{2} - \frac{1}{2}\log_2(1-3P_1) < 0$, and $-\frac{1}{2} - \frac{1}{2}\log_2(3P_1) > 0$. Hence, we conclude that when $P_2 = \frac{2}{3}$ and $0 \le P_1 < \frac{1}{6}$, using $(n-1)$ type $2+1$ type 1 quantizers always outperform $\gamma_{n,2}$. Since Figure 3.1 indicates that $\gamma_{n,2}$ is the optimal IQS between the two margins of $\gamma_{n,1} = \gamma_{n,2}$ and $\gamma_{n,2} = \gamma_{n,3}$ for $0 \le P_1 \le \frac{1}{3}$ and $\frac{1}{3} \le P_2 \le 1$, we can then decide numerically that for the line segment decided by $P_2 = \frac{2}{3}$ and $\frac{5}{64} \le P_1 < \frac{1}{6}$, the IQS is only suboptimal.

Note that when $P_1 = \frac{1}{6}$, no integer satisfies both (3.16) and (3.17); hence, using $(n-1)$ type $2+1$ type 1 quantizers have the same performance as $\gamma_{n,2}$. In such case, we can no longer claim that the IQS is only suboptimal.

D) Line Segment 4

We now proceed to prove the validity of line segment 4. For $P_2 = 2/3$, the two gamma functions are given by:

$$\begin{aligned}
\bar{r}(\pi) &= \left[P_2\pi \ \wedge \ \frac{1}{3}(1-\pi)\right] + \left[(1-P_2)\pi \ \wedge \ \frac{2}{3}(1-\pi)\right] \\
&= \left[\frac{2}{3}\pi \ \wedge \ \frac{1}{3}(1-\pi)\right] + \left[\frac{1}{3}\pi \ \wedge \ \frac{2}{3}(1-\pi)\right] \\
&= \begin{cases} \frac{2}{3}\pi + \frac{1}{3}\pi, & 0 \le \pi < \frac{1}{3} \\ \frac{1}{3}(1-\pi) + \frac{1}{3}\pi, & \frac{1}{3} \le \pi < \frac{2}{3} \\ \frac{1}{3}(1-\pi) + \frac{2}{3}(1-\pi), & \frac{2}{3} \le \pi \le 1 \end{cases} \\
&= \begin{cases} \pi, & 0 \le \pi < \frac{1}{3} \\ \frac{1}{3}, & \frac{1}{3} \le \pi < \frac{2}{3} \\ 1-\pi, & \frac{2}{3} \le \pi \le 1 \end{cases}
\end{aligned}$$

and for $P_{12} = P_1 + P_2 = P_1 + \frac{2}{3}$,

$$\hat{r}(\pi) = \left[P_{12}\pi \ \wedge \ \frac{2}{3}(1-\pi)\right] + \left[(1-P_{12})\pi \ \wedge \ \frac{1}{3}(1-\pi)\right].$$

It can be verified that $\frac{2}{3P_{12}+2} < \frac{1}{4-3P_{12}}$; hence,

$$\begin{aligned}
\hat{r}(\pi) &= \left[P_{12}\pi \ \wedge \ \frac{1}{3}(1-\pi)\right] + \left[(1-P_{12})\pi \ \wedge \ \frac{2}{3}(1-\pi)\right] \\
&= \begin{cases} P_{12}\pi + (1-P_{12})\pi, & 0 \le \pi < \frac{2}{3P_{12}+2} \\ \frac{2}{3}(1-\pi) + (1-P_{12})\,\pi, & \frac{2}{3P_{12}+2} \le \pi < \frac{1}{4-3P_{12}} \\ \frac{2}{3}(1-\pi) + \frac{1}{3}(1-\pi), & \frac{1}{4-3P_{12}} \le \pi \le 1 \end{cases} \\
&= \begin{cases} \pi, & 0 \le \pi < \frac{2}{3P_{12}+2} \\ \frac{2}{3} + \left(\frac{1}{3} - P_{12}\right)\pi, & \frac{2}{3P_{12}+2} \le \pi < \frac{1}{4-3P_{12}} \\ 1-\pi, & \frac{1}{4-3P_{12}} \le \pi \le 1 \end{cases}
\end{aligned}$$

The two ranges that $\hat{\gamma}(\pi) \neq \bar{\gamma}(\pi)$ are $(\frac{1}{3}, \frac{1}{3P_{12}-1})$ and $(\frac{1}{3P_{12}-1}, \frac{1}{4-3P_{12}})$, where $\hat{\gamma}(\pi)$ is larger than $\bar{\gamma}(\pi)$ in the former range but is smaller than $\bar{\gamma}(\pi)$ in the latter range. This results in the derivation that

$$\frac{1}{3} < \frac{1}{1+2^{n-1-2l}} < \frac{1}{3P_{12}-1} \quad \text{and} \quad \frac{1}{3P_{12}-1} < \frac{1}{1+2^{n-1-2l}} < \frac{1}{4-3P_{12}},$$

or equivalently,

$$\frac{n}{2} - 1 < l < \frac{n}{2} - \frac{1}{2} - \frac{1}{2}\log_2(3P_{12}-2) \tag{3.18}$$

and

$$\frac{n}{2} - \frac{1}{2} - \frac{1}{2}\log_2(3P_{12}-2) < l < \frac{n}{2} - \frac{1}{2} - \frac{1}{2}\log_2(3-3P_{12}). \tag{3.19}$$

Suppose $n = 2k$ is even. Therefore, if

$$k - \frac{1}{2} - \frac{1}{2}\log_2(3P_{12}-2) < k \quad \left(\text{i.e., } P_{12} > \frac{5}{6}, \text{ or equivalently } P_1 > \frac{1}{6}\right),$$

then no integer l satisfies (3.18). Note that $P_1 > \frac{1}{6}$ implies that $-\frac{1}{2} - \frac{1}{2}\log_2(3P_{12}-2) < 0$, and $-\frac{1}{2} - \frac{1}{2}\log_2(3-3P_{12}) > 0$. Hence, we conclude that when $P_2 = \frac{2}{3}$ and $\frac{1}{6} < P_1 \le 1$, using $(n-1)$ type $2+1$ type 3 quantizers always outperform $\gamma_{n,2}$. Since Figure 3.1 indicates that $\gamma_{n,2}$ is the optimal IQS between the two margins of $\gamma_{n,1} = \gamma_{n,2}$ and $\gamma_{n,2} = \gamma_{n,3}$ for $0 \le P_1 \le \frac{1}{3}$ and $\frac{1}{3} \le P_2 \le 1$, we can then decide numerically that for the line segment decided by $P_2 = \frac{2}{3}$ and $\frac{1}{6} \le P_1 < \frac{49}{192}$, the IQS is only suboptimal.

Note that when $P_1 = \frac{1}{6}$, no integer satisfies both (3.18) and (3.19); hence, using $(n-1)$ type 2 + 1 type 3 quantizers have the same performance as $\gamma_{n,2}$. In such case, we can no longer claim that the IQS is only suboptimal.

E) Line Segment 5

Our next proof is for line segment 5. For $P_1 + P_2 = 3/4$, the two gamma functions are given by:

$$\begin{aligned}
\bar{r}(\pi) &= \left[\frac{3}{4}\pi \ \wedge \ \frac{2}{3}(1-\pi)\right] + \left[\frac{1}{4}\pi \ \wedge \ \frac{1}{3}(1-\pi)\right] \\
&= \begin{cases} \frac{3}{4}\pi + \frac{1}{4}\pi, & 0 \le \pi < \frac{8}{17} \\ \frac{2}{3}(1-\pi) + \frac{1}{4}\pi, & \frac{8}{17} \le \pi < \frac{4}{7} \\ \frac{2}{3}(1-\pi) + \frac{1}{3}(1-\pi), & \frac{4}{7} \le \pi \le 1 \end{cases} \\
&= \begin{cases} \pi, & 0 \le \pi < \frac{2}{5} \\ \frac{2}{3} - \frac{5}{12}\pi, & \frac{2}{5} \le \pi < \frac{4}{7} \\ 1-\pi, & \frac{4}{7} \le \pi \le 1 \end{cases}
\end{aligned}$$

and for $P_1 \le 3/8$ such that $\frac{2}{5-3P_1} \le \frac{1}{3P_1+1}$,

$$\begin{aligned}
\hat{r}(\pi) &= \left[P_1\pi \ \wedge \ \frac{1}{3}(1-\pi)\right] + \left[(1-P_1)\pi \ \wedge \ \frac{2}{3}(1-\pi)\right] \\
&= \begin{cases} P_1\pi + (1-P_1)\pi, & 0 \le \pi < \frac{2}{5-3P_2} \\ P_1\pi + \frac{2}{3}(1-\pi), & \frac{2}{5-3P_1} \le \pi < \frac{1}{3P_1+1} \\ \frac{1}{3}(1-\pi) + \frac{2}{3}(1-\pi), & \frac{1}{3P_1+1} \le \pi \le 1 \end{cases} \\
&= \begin{cases} \pi, & 0 \le \pi < \frac{2}{5-3P_1} \\ \frac{2}{3} + \left(P_1 - \frac{2}{3}\right)\pi, & \frac{2}{5-3P_1} \le \pi < \frac{1}{3P_1+1} \\ 1-\pi, & \frac{1}{3P_1+1} \le \pi \le 1 \end{cases}
\end{aligned}$$

The only range that $\hat{\gamma}(\pi) > \bar{\gamma}(\pi)$ is $(\frac{8}{17}, \frac{1}{1+3P_1})$. By (2.3), we derive

$$\begin{aligned}
\pi &= \frac{P_{\bar{g}}(u_1^{n-1})}{P_{\bar{g}}(u_1^{n-1}) + Q_{\bar{g}}(u_1^{n-1})} \\
&= \frac{(\frac{3}{4})^l(\frac{1}{4})^{n-l-1}}{(\frac{3}{4})^l(\frac{1}{4})^{n-l-1} + (\frac{2}{3})^l(\frac{1}{3})^{n-l-1}} \\
&= \frac{1}{1 + (\frac{8}{9})^l(\frac{4}{3})^{n-l-1}}.
\end{aligned}$$

Hence, to check wether the IQS is suboptimal, we examine:

$$\frac{8}{17} < \frac{1}{1+(\frac{8}{9})^l(\frac{4}{3})^{n-l-1}} < \frac{1}{3P_1-1},$$

or equivalently,

$$\frac{\log_2(3P_1)+(1-n)\log_2(\frac{4}{3})}{\log_2(\frac{2}{3})} < l < \frac{\log_2(\frac{9}{8})+(1-n)\log_2(\frac{4}{3})}{\log_2(\frac{2}{3})} = \alpha n - 1. \tag{3.20}$$

where $\alpha = \frac{2-\log_2(3)}{1-\log_2(3)} \approx 0.7095$ is an irrational number.

Now, if we place probability mass $1/N$ at points $\{\alpha n - \lfloor \alpha n \rfloor\}_{n=1}^{N}$ to form a probability measure μ_n, then by the theory about the so-called *uniformly distributed modulo 1* [6], we have μ_n converges in distribution to μ, where μ is a uniform distribution over $(0, 1]$. This indicates as long as

$$P_1 < \frac{3}{8},$$

there exists integer l satisfying (3.20) for infinitely many n. Hence, we conclude that when $0 \leq P_1 < \frac{8}{3}$ subject to $P_1 + P_2 = \frac{3}{4}$, using $(n-1)$ type $3+1$ type 1 quantizers always outperform $\gamma_{n,3}$. Since Figure 3.1 indicates that $\gamma_{n,3}$ is the optimal IQS between the two margins of $\gamma_{n,1} = \gamma_{n,3}$ and $\gamma_{n,2} = \gamma_{n,3}$, we can then decide numerically that for the line segment decided by $P_1 + P_2 = \frac{3}{4}$, $\frac{21}{64} \leq P_1 < \frac{3}{8}$ and $\frac{3}{8} < P_2 \leq \frac{27}{64}$, the IQS is suboptimal infinitely often in n.

Note that when $P_1 = \frac{3}{8}$, no integer satisfies (3.20); hence, using $(n-1)$ type $3+1$ type 1 quantizers have the same performance as $\gamma_{n,3}$. In such case, we can no longer claim that the IQS is only suboptimal.

F) Line Segment 6

We now turn to the last proof about line segment 6. For $P_{12} = P_1 + P_2 = 3/4$, the two

gamma functions are given by:

$$\begin{aligned}
\bar{r}(\pi) &= \left[P_{12}\pi \ \wedge \ \frac{2}{3}(1-\pi)\right] + \left[(1-P_{12})\pi \ \wedge \ \frac{1}{3}(1-\pi)\right] \\
&= \left[\frac{3}{4}\pi \ \wedge \ \frac{2}{3}(1-\pi)\right] + \left[\frac{1}{4}\pi \ \wedge \ \frac{1}{3}(1-\pi)\right] \\
&= \begin{cases} \frac{3}{4}\pi + \frac{1}{4}\pi, & 0 \le \pi < \frac{8}{17} \\ \frac{2}{3}(1-\pi) + \frac{1}{4}\pi, & \frac{8}{17} \le \pi < \frac{4}{7} \\ \frac{2}{3}(1-\pi) + \frac{1}{3}(1-\pi), & \frac{4}{7} \le \pi \le 1 \end{cases} \\
&= \begin{cases} \pi, & 0 \le \pi < \frac{2}{5} \\ \frac{2}{3} - \frac{5}{12}\pi, & \frac{2}{5} \le \pi < \frac{4}{7} \\ 1-\pi, & \frac{4}{7} \le \pi \le 1 \end{cases}
\end{aligned}$$

and for $P_2 \le \frac{3}{8}$ such that $\frac{2}{5-3P_2} \le \frac{1}{3P_2+1}$,

$$\begin{aligned}
\hat{r}(\pi) &= \left[P_2\pi \ \wedge \ \frac{1}{3}(1-\pi)\right] + \left[(1-P_2)\pi \ \wedge \ \frac{2}{3}(1-\pi)\right] \\
&= \begin{cases} P_2\pi + (1-P_2)\pi, & 0 \le \pi < \frac{2}{5-3P_2} \\ P_2\pi + \frac{2}{3}(1-\pi), & \frac{2}{5-3P_2} \le \pi < \frac{1}{3P_2+1} \\ \frac{1}{3}(1-\pi) + \frac{2}{3}(1-\pi), & \frac{1}{3P_2+1} \le \pi \le 1 \end{cases} \\
&= \begin{cases} \pi, & 0 \le \pi < \frac{2}{5-3P_2} \\ \frac{2}{3} + \left(P_2 - \frac{2}{3}\right)\pi, & \frac{2}{5-3P_2} \le \pi < \frac{1}{3P_2+1} \\ 1-\pi, & \frac{1}{3P_2+1} \le \pi \le 1 \end{cases}
\end{aligned}$$

The only one range that $\hat{\gamma}(\pi) > \bar{\gamma}(\pi)$ is again $(\frac{8}{17}, \frac{1}{1+3P_2})$. Derive from (2.3) that

$$\begin{aligned}
\pi &= \frac{P_{\bar{g}}(u_1^{n-1})}{P_{\bar{g}}(u_1^{n-1}) + Q_{\bar{g}}(u_1^{n-1})} \\
&= \frac{(\frac{3}{4})^l(\frac{1}{4})^{n-l-1}}{(\frac{3}{4})^l(\frac{1}{4})^{n-l-1} + (\frac{2}{3})^l(\frac{1}{3})^{n-l-1}} \\
&= \frac{1}{1 + (\frac{8}{9})^l(\frac{4}{3})^{n-l-1}}.
\end{aligned}$$

Hence, to examine whether the IQS is suboptimal or not, we continue to derive

$$\frac{8}{17} < \frac{1}{1 + (\frac{8}{9})^l(\frac{4}{3})^{n-l-1}} < \frac{1}{3P_2 - 1},$$

or equivalently,

$$\frac{\log_2(3P_2) + (1-n)\log_2(\frac{4}{3})}{\log_2(\frac{2}{3})} < l < \frac{\log_2(\frac{9}{8}) + (1-n)\log_2(\frac{4}{3})}{\log_2(\frac{2}{3})} = \alpha n - 1, \tag{3.21}$$

where $\alpha = \frac{2-\log_2(3)}{1-\log_2(3)} \approx 0.7095$ is an irrational number.

Again, if we place probability mass $1/N$ at points $\{\alpha n - \lfloor \alpha n \rfloor\}_{n=1}^{N}$ to form a probability measure μ_n, then by the theory about the so-called *uniformly distributed modulo 1* [6], we have μ_n converges in distribution to μ, where μ is a uniform distribution over $(0, 1]$. This indicates as long as

$$P_2 < \frac{3}{8},$$

there exists integer l satisfying (3.21) for infinitely many n. Hence, we conclude that when $0 \leq P_2 < \frac{8}{3}$ subject to $P_1 + P_2 = \frac{3}{4}$, using $(n-1)$ type $3+1$ type 2 quantizers always outperform $\gamma_{n,3}$. Since Figure 3.1 indicates that $\gamma_{n,3}$ is the optimal IQS between the two margins of $\gamma_{n,1} = \gamma_{n,3}$ and $\gamma_{n,2} = \gamma_{n,3}$, we can then decide numerically that for the line segment decided by $P_1 + P_2 = \frac{3}{4}$, $\frac{3}{8} \leq P_1 < \frac{27}{64}$ and $\frac{21}{64} \leq P_2 < \frac{3}{8}$, the IQS is suboptimal infinitely often in n.

Note that when $P_2 = \frac{3}{8}$, no integer satisfies (3.21); hence, using $(n-1)$ type $3+1$ type 2 quantizers have the same performance as $\gamma_{n,3}$. In such case, we can no longer claim that the IQS is only suboptimal.

3.2.3 Case 2: Non-Uniform Alternative Hypothesis Distribution

We also examine a case that equips with non-uniform alternative hypothesis distribution. The statistics for local observations in $\{a_1, a_2, a_3\}$ is denoted as follows:

$$\begin{cases} \Pr(a_1|H_0) = P_1 \\ \Pr(a_2|H_0) = P_2 \\ \Pr(a_3|H_0) = 1 - P_1 - P_2 \end{cases} \quad \text{and} \quad \begin{cases} \Pr(a_1|H_1) = \frac{1}{4} \\ \Pr(a_2|H_1) = \frac{1}{4} \\ \Pr(a_3|H_1) = \frac{1}{2} \end{cases}$$

The above equations can also be listed in a tabular form below.

y	a_1	a_2	a_3
$\Pr(y\|H_0)$	P_1	P_2	$1-P_1-P_2$
$\Pr(y\|H_1)$	$\frac{1}{4}$	$\frac{1}{4}$	$\frac{1}{2}$

Similar to the previous case, we can perform binary quantizer and yields three LRQ types. The corresponding post-quantization distributions are listed in Table 3.3.

Table 3.3: For convenience, we denote $P_3 = P_1 + P_2$.

u	0	1
$P_{g_1}(u)$	P_1	$1-P_1$
$Q_{g_1}(u)$	$\frac{1}{4}$	$\frac{3}{4}$
u	0	1
$P_{g_2}(u)$	P_2	$1-P_2$
$Q_{g_2}(u)$	$\frac{1}{4}$	$\frac{3}{4}$
u	0	1
$P_{g_3}(u)$	P_3	$1-P_3$
$Q_{g_3}(u)$	$\frac{1}{2}$	$\frac{1}{2}$

The results are very similar to that for the first case. The picture of the optimal IQS region is also divided into six areas and the margins of the six areas must be decided numerically. However, since the areas are more messy than Case 1 due to non-uniformity of the alternative hypothesis distribution, no conclusive results are obtained; we therefore defer this part as a future work.

Chapter 4

Simulation Results

In this chapter, numerical and simulation results are provided to confirm and demonstrate the derivations in Chapter 3. For better readability, simulation results are summarized in Section 4.1, and discussions regarding them are given in Section 4.2.

4.1 Summary of Numerical and Simulation Results

We first introduce the system setting of the following simulations.

1. Figures 4.1–4.12 show the resulting error probabilities for all possible combinations of the LRQs introduced in Section 3.1.

   (a) What presented in Figures 4.1 - 4.4 are the performances of the hypothesis setting below.

y	a_1	a_2	a_3
$\Pr(y\|H_0)$	$\frac{1}{12}$	$\frac{1}{4}$	$\frac{2}{3}$
$\Pr(y\|H_1)$	$\frac{1}{3}$	$\frac{1}{3}$	$\frac{1}{3}$

   After binary quantization, it will result in two nontrivial LRQs as shown in Table 4.1.

Table 4.1:

u	0	1
$P_{\hat{g}}(u) = \Pr(u\|H_0)$	$\frac{1}{12}$	$\frac{11}{12}$
$Q_{\hat{g}}(u) = \Pr(u\|H_1)$	$\frac{1}{3}$	$\frac{2}{3}$
u	0	1
$P_{\bar{g}}(u) = \Pr(u\|H_0)$	$\frac{1}{3}$	$\frac{2}{3}$
$Q_{\bar{g}}(u) = \Pr(u\|H_1)$	$\frac{2}{3}$	$\frac{1}{3}$

In our experiment, we will base on the IQS, where all sensors use $\bar{g}$ as their local quantizers, and gradually increase the number of sensors that use LRQ $\hat{g}$, for which the number is indicated by the x-axis. We can observe that the performance basically improves but not monotonically when the number of $\hat{g}$ LRQ sensors increase. It hints that the optimal NQS only use very few number (actually only one in Figures 4.1 and4.10)of $\bar{g}$ quantizers but is nearly close to an identical quantizer system.

(b) Again, what presented in Figures 4.5 - 4.8 are the performances of the hypothesis setting below.

y	a_1	a_2	a_3
$\Pr(y\|H_0)$	$\frac{1}{9}$	$\frac{4}{9}$	$\frac{4}{9}$
$\Pr(y\|H_1)$	$\frac{1}{3}$	$\frac{1}{3}$	$\frac{1}{3}$

After binary quantization, it will result in two nontrivial LRQs as shown in Table 4.2.

Similar to the previous experiment, we start from the IQS that uses unanimously $\bar{g}$ and then gradually increase the number of sensors using LRQ $\hat{g}$. Different form the previous case, the performance monotonically degrades and hence the initial IQS is actually the optimal system.

Table 4.2:

u	0	1
$P_{\hat{g}}(u) = \Pr(u\|H_0)$	$\frac{1}{9}$	$\frac{8}{9}$
$Q_{\hat{g}}(u) = \Pr(u\|H_1)$	$\frac{1}{3}$	$\frac{2}{3}$
u	0	1
$P_{\bar{g}}(u) = \Pr(u\|H_0)$	$\frac{5}{9}$	$\frac{4}{9}$
$Q_{\bar{g}}(u) = \Pr(u\|H_1)$	$\frac{2}{3}$	$\frac{1}{3}$

(c) What presented in Figures 4.9 - 4.12 are the performances of hypothesis distribution pair indicated below.

y	a_1	a_2	a_3
$\Pr(y\|H_0)$	$\frac{1}{23}$	$\frac{1}{23}$	$\frac{21}{23}$
$\Pr(y\|H_1)$	$\frac{1}{3}$	$\frac{1}{3}$	$\frac{1}{3}$

After binary quantization, it will result in two nontrivial LRQs as shown in Table 4.3.

Table 4.3:

u	0	1
$P_{\hat{g}}(u) = \Pr(u\|H_0)$	$\frac{1}{23}$	$\frac{22}{23}$
$Q_{\hat{g}}(u) = \Pr(u\|H_1)$	$\frac{1}{3}$	$\frac{2}{3}$
u	0	1
$P_{\bar{g}}(u) = \Pr(u\|H_0)$	$\frac{2}{23}$	$\frac{21}{23}$
$Q_{\bar{g}}(u) = \Pr(u\|H_1)$	$\frac{2}{3}$	$\frac{1}{3}$

Parallel to the previous case, we also observe a monotonic behavior of the performances when we increase the number of sensors using LRQ $\hat{g}$. However, the detection errors decrease instead of increase in this case. Hence, the IQS, where

all sensors use LRQ $\hat{g}$, is the globally optimal design.

2. Figures 4.13 and 4.14 show the area, of which local LRQ gives the best IQS. The three possible LRQs are termed type 1, type 2 and type 3, depending on which of the local observations in $\{a_1, a_2, a_3\}$ is isolated as specified the same as in Table 3.1. Different colors are adopted for different areas according to:

   type 1 gives the best IQS : dark gray
   type 2 gives the best IQS : gray
   type 3 gives the best IQS : light gray

   The local hypothesis setting in Figure 4.13 is as follows.

y	a_1	a_2	a_3
$\Pr(y\|H_0)$	P_1	P_2	$1-P_1-P2$
$\Pr(y\|H_1)$	$\frac{1}{3}$	$\frac{1}{3}$	$\frac{1}{3}$

   The local hypothesis setting in Figure 4.14 is given below.

y	a_1	a_2	a_3
$\Pr(y\|H_0)$	P_1	P_2	$1-P_1-P_2$
$\Pr(y\|H_1)$	$\frac{1}{4}$	$\frac{1}{4}$	$\frac{1}{2}$

   We specifically try an odd number of sensors (e.g., 39) and an even number of sensors (e.g., 60) in our experiment to see whether the patterns alternate according to odd or even number of sensors.

3. Figures 4.15 and 4.16 show the areas, in which the NQS with one different local LRQ improves the best IQS. When such an improvement occurs, we will use the following

colors to indicate it:

$$\begin{aligned}
&(n-1) \text{ type } 1 + 1 \text{ type } 2 : \text{dark red} \\
&(n-1) \text{ type } 1 + 1 \text{ type } 3 : \text{red} \\
&(n-1) \text{ type } 2 + 1 \text{ type } 1 : \text{dark green} \\
&(n-1) \text{ type } 2 + 1 \text{ type } 3 : \text{green} \\
&(n-1) \text{ type } 3 + 1 \text{ type } 1 : \text{dark blue} \\
&(n-1) \text{ type } 3 + 1 \text{ type } 2 : \text{blue}
\end{aligned} \tag{4.1}$$

In this experiment, the distribution of the pre-quantization local observation is given by:

y	a_1	a_2	a_3
$\Pr(y\|H_0)$	P_1	P_2	$1-P_1-P_2$
$\Pr(y\|H_1)$	$\frac{1}{3}$	$\frac{1}{3}$	$\frac{1}{3}$

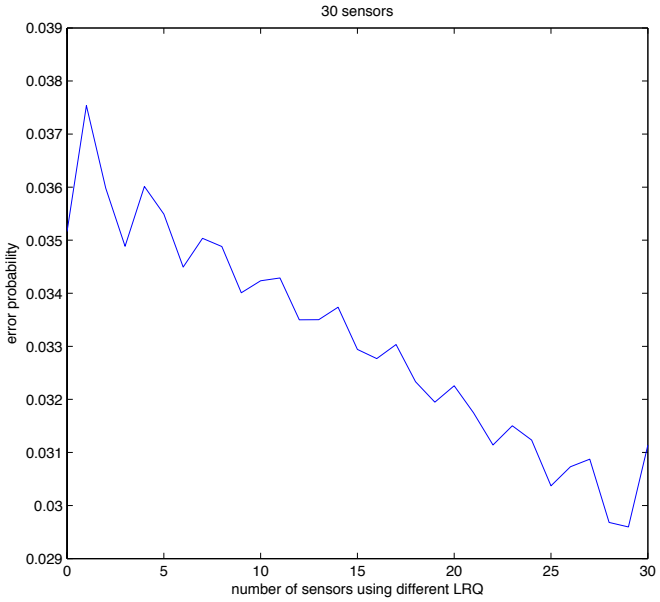

(a)

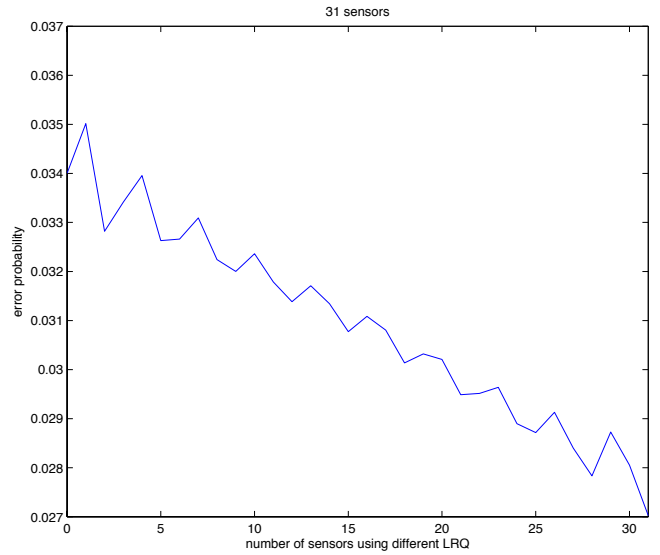

(b)

Figure 4.1: Detect errors for the LRQs in Table 4.1. The x-axis indicates the number of sensors that use LRQ $\hat{g}$. As indicated on top of the plots, the total numbers of sensors are respectively 30 and 31 in (a) and (b).

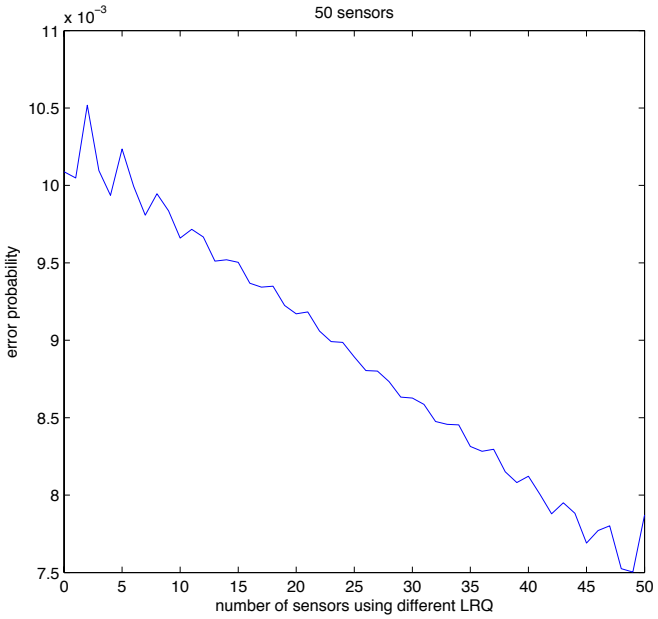

(a)

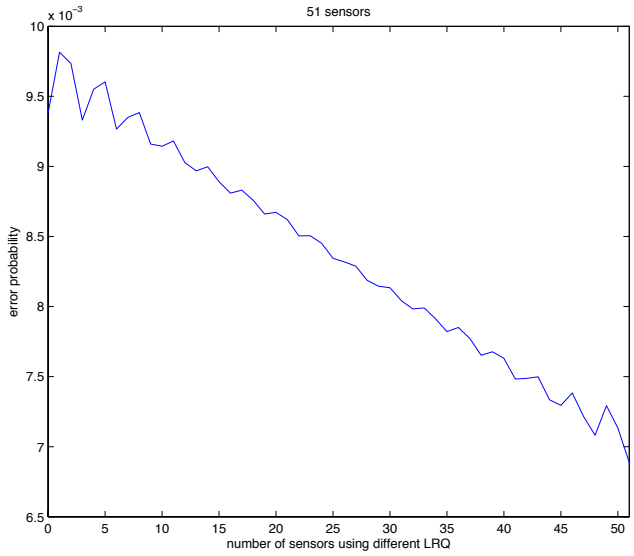

(b)

Figure 4.2: Detect errors for the LRQs in Table 4.1. The x-axis indicates the number of sensors that use LRQ $\hat{g}$. As indicated on top of the plots, the total numbers of sensors are respectively 50 and 51 in (a) and (b).

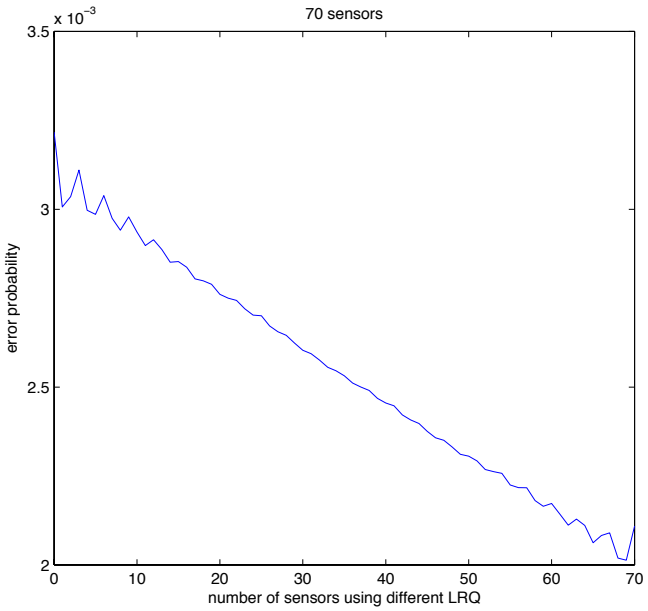

(a)

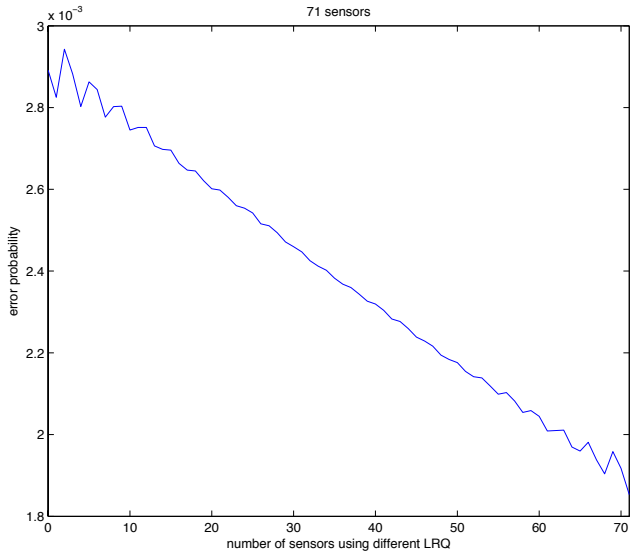

(b)

Figure 4.3: Detect errors for the LRQs in Table 4.1. The x-axis indicates the number of sensors that use LRQ $\hat{g}$. As indicated on top of the plots, the total numbers of sensors are respectively 70 and 71 in (a) and (b).

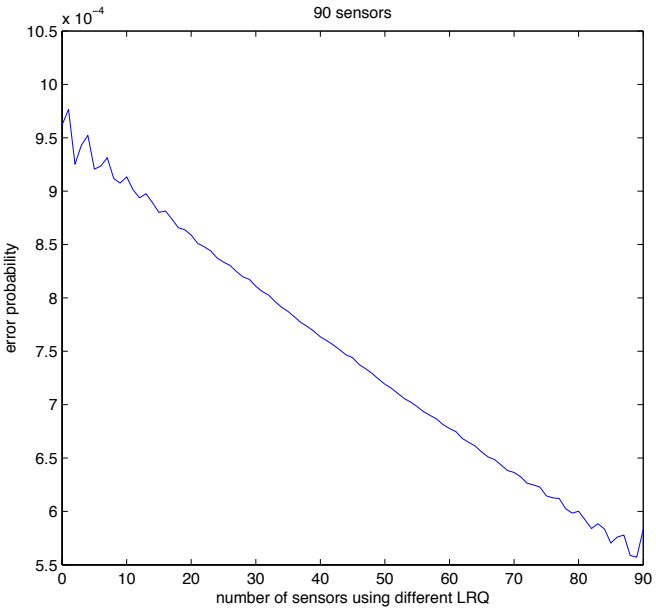

(a)

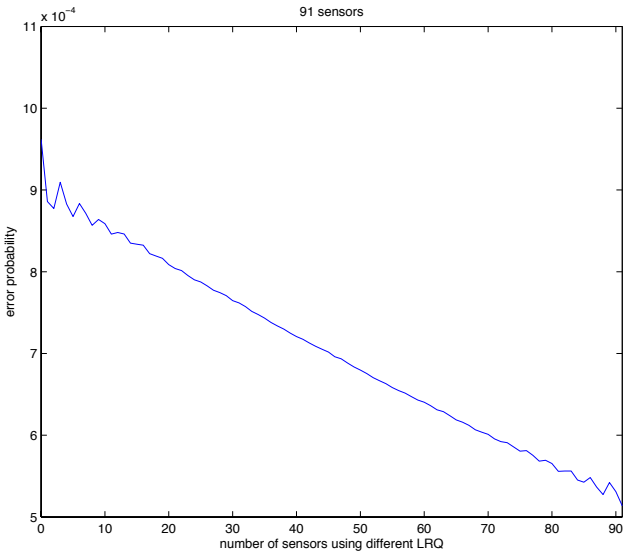

(b)

Figure 4.4: Detect errors for the LRQs in Table 4.1. The x-axis indicates the number of sensors that use LRQ $\hat{g}$. As indicated on top of the plots, the total numbers of sensors are respectively 90 and 91 in (a) and (b).

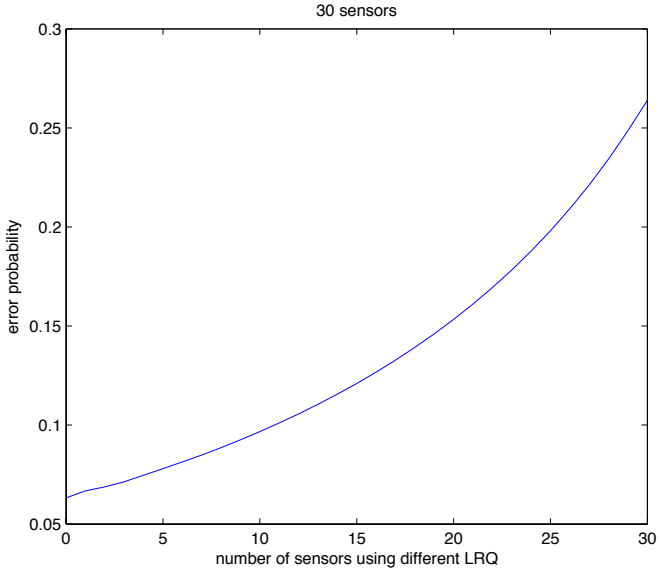

(a)

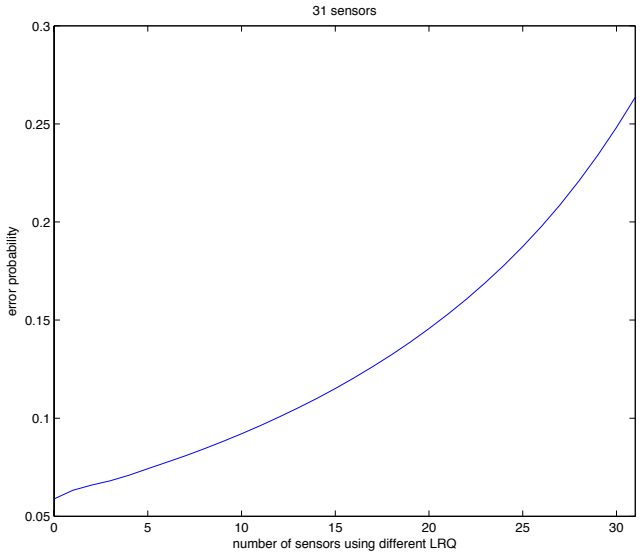

(b)

Figure 4.5: Detect errors for the LRQs in Table 4.2. The x-axis indicates the number of sensors that use LRQ $\hat{g}$. As indicated on top of the plots, the total numbers of sensors are respectively 30 and 31 in (a) and (b).

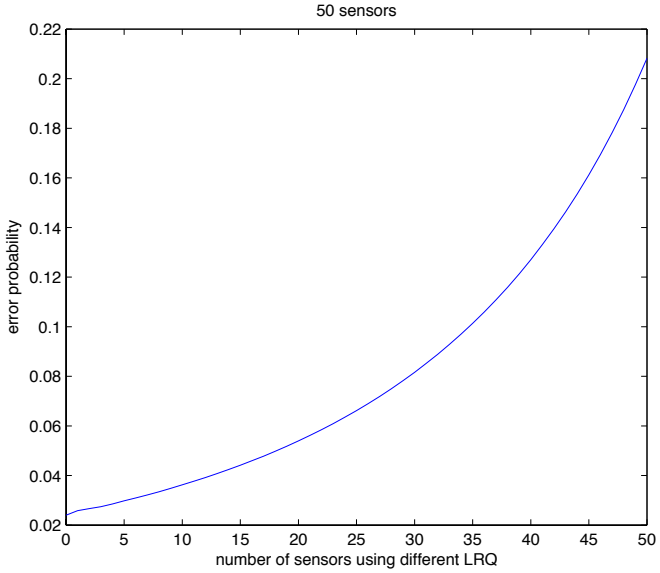

(a)

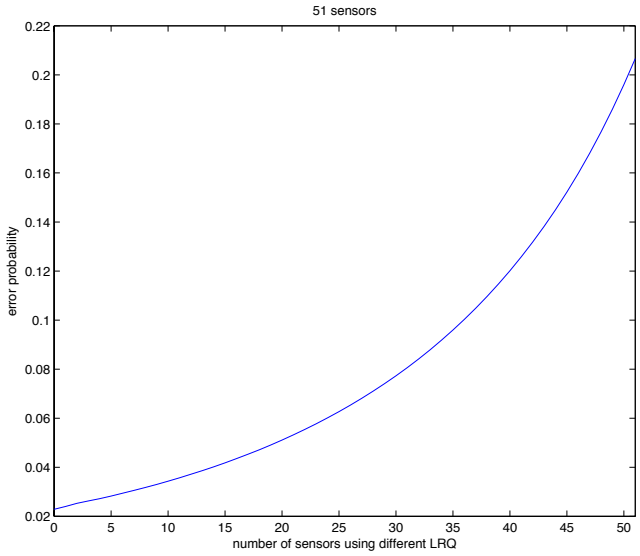

(b)

Figure 4.6: Detect errors for the LRQs in Table 4.2. The x-axis indicates the number of sensors that use LRQ $\hat{g}$. As indicated on top of the plots, the total numbers of sensors are respectively 50 and 51 in (a) and (b).

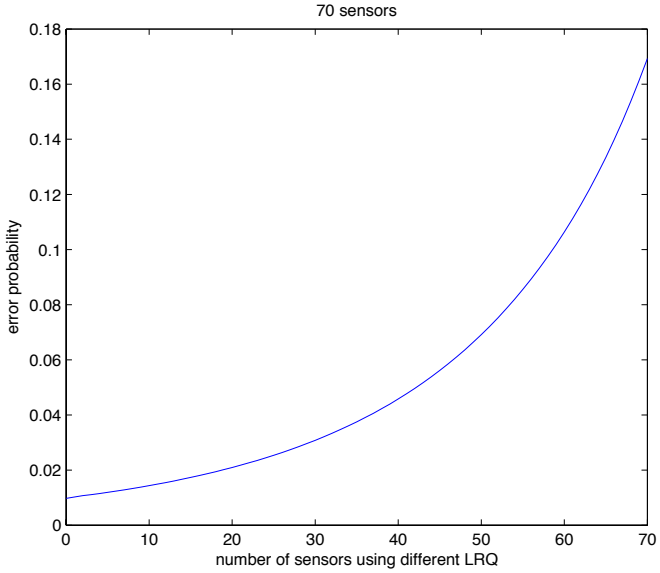

(a)

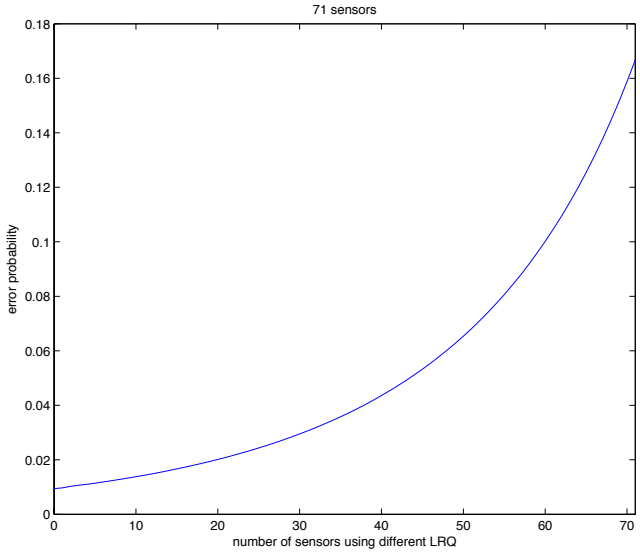

(b)

Figure 4.7: Detect errors for the LRQs in Table 4.2. The x-axis indicates the number of sensors that use LRQ $\hat{g}$. As indicated on top of the plots, the total numbers of sensors are respectively 70 and 71 in (a) and (b).

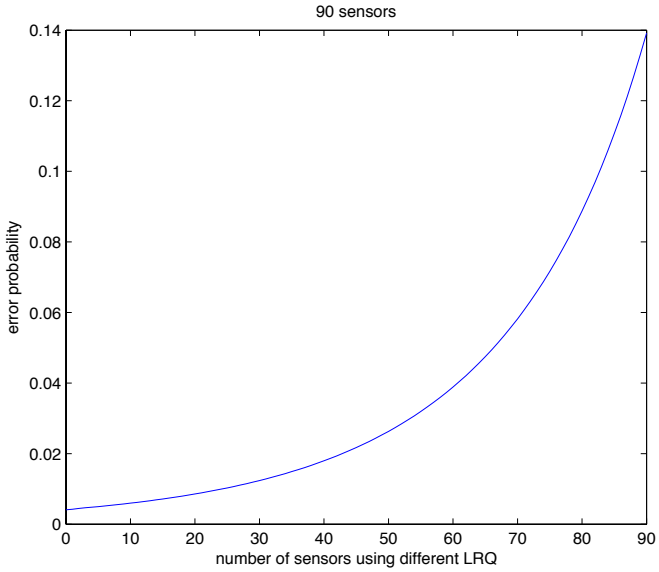

(a)

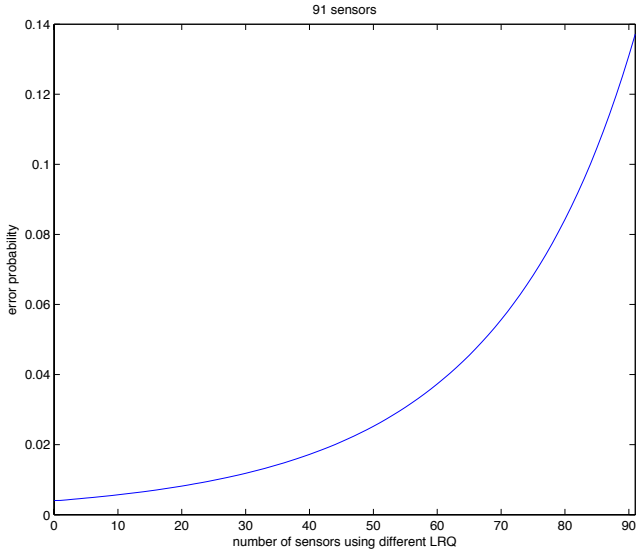

(b)

Figure 4.8: Detect errors for the LRQs in Table 4.2. The x-axis indicates the number of sensors that use LRQ $\hat{g}$. As indicated on top of the plots, the total numbers of sensors are respectively 90 and 91 in (a) and (b).

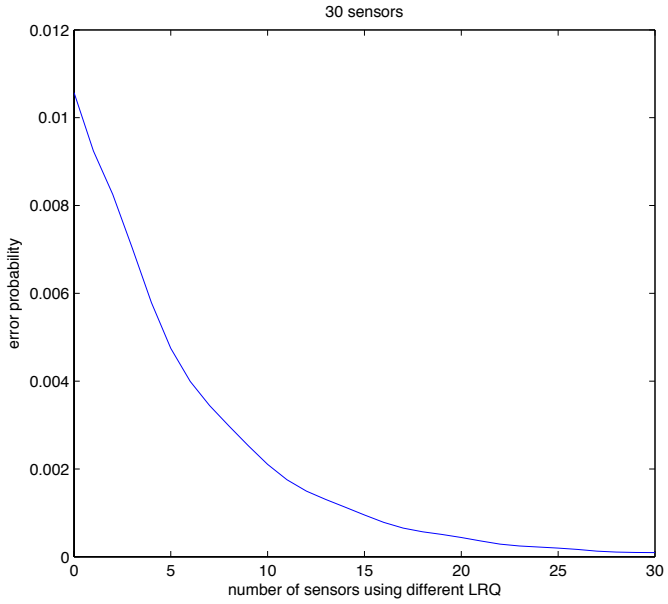

(a)

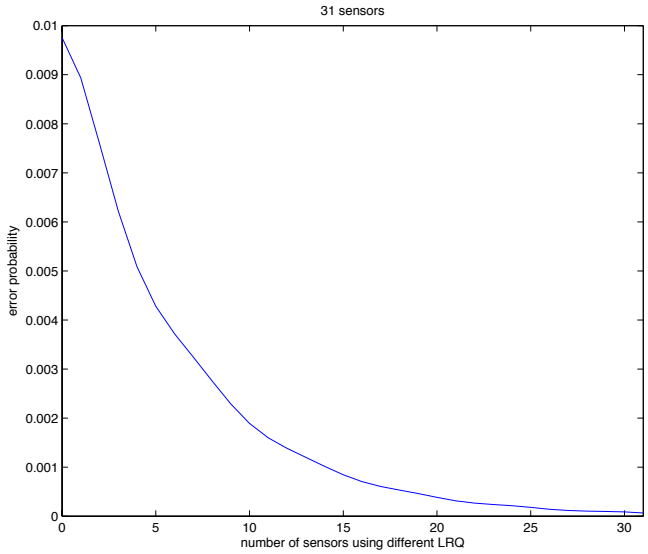

(b)

Figure 4.9: Detection errors for the LRQs in Table 4.3. The x-axis indicates the number of sensors that use LRQ $\hat{g}$. As indicated on top of the plots, the numbers of sensors are respectively 30 and 31 in (a) and (b).

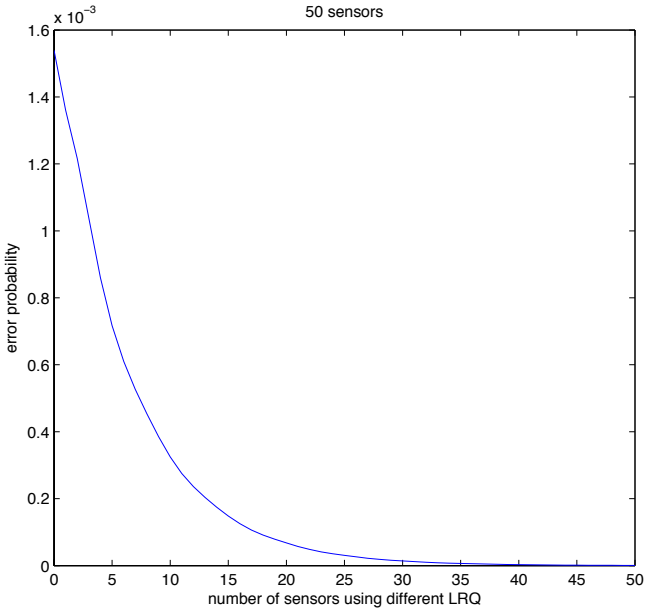

(a)

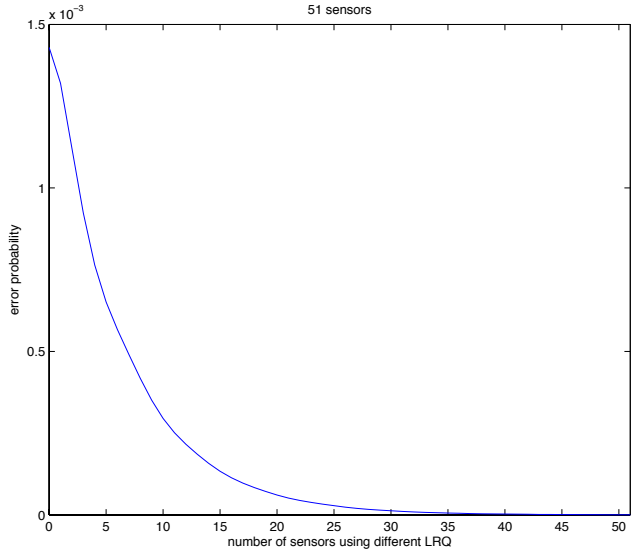

(b)

Figure 4.10: Detection errors for the LRQs in Table 4.3. The x-axis indicates the number of sensors that use LRQ $\hat{g}$. As indicated on top of the plots, the numbers of sensors are respectively 50 and 51 in (a) and (b).

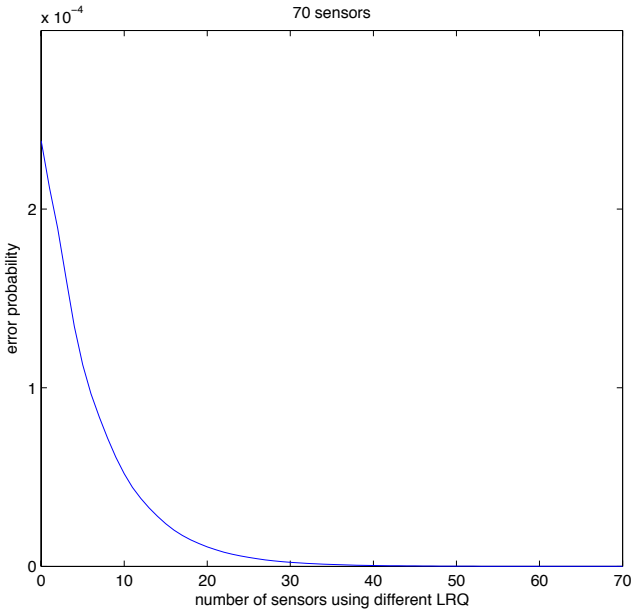

(a)

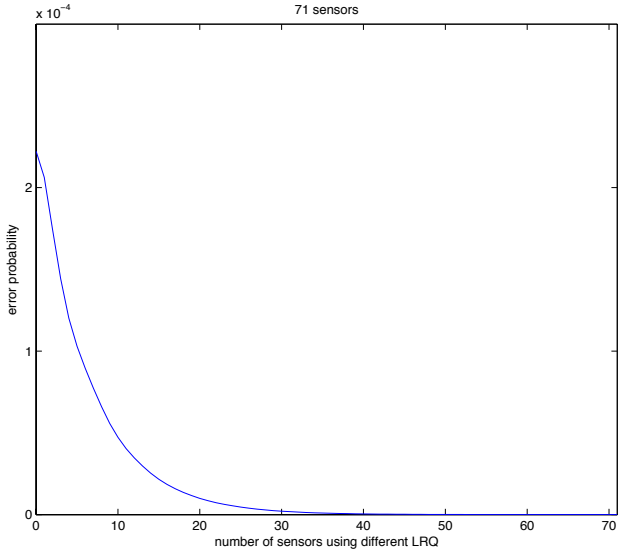

(b)

Figure 4.11: Detect errors for the LRQs in Table 4.2. The x-axis indicates the number of sensors that use LRQ $\hat{g}$. As indicated on top of the plots, the total numbers of sensors are respectively 70 and 71 in (a) and (b).

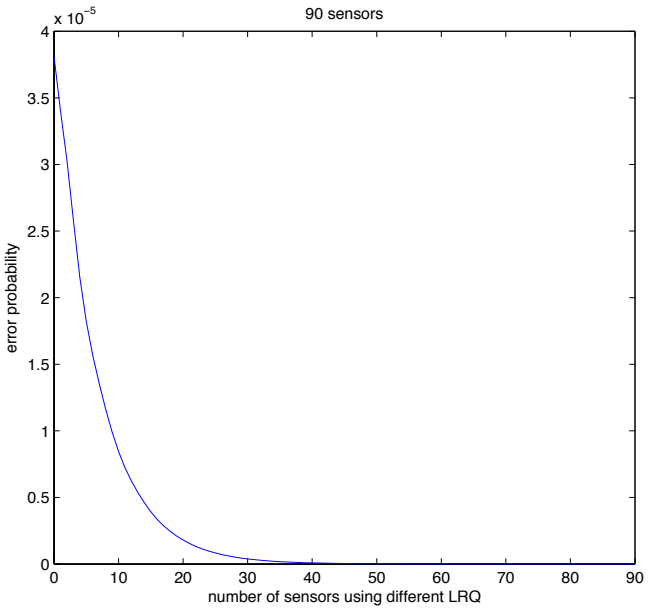

(a)

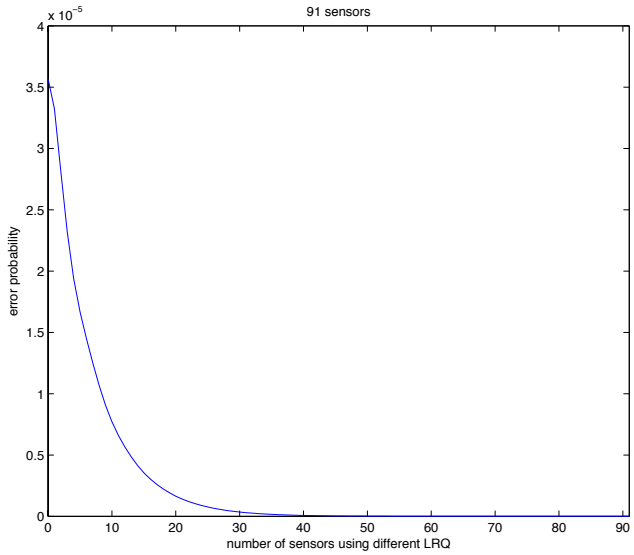

(b)

Figure 4.12: Detect errors for the LRQs in Table 4.2. The x-axis indicates the number of sensors that use LRQ $\hat{g}$. As indicated on top of the plots, the total numbers of sensors are respectively 90 and 91 in (a) and (b).

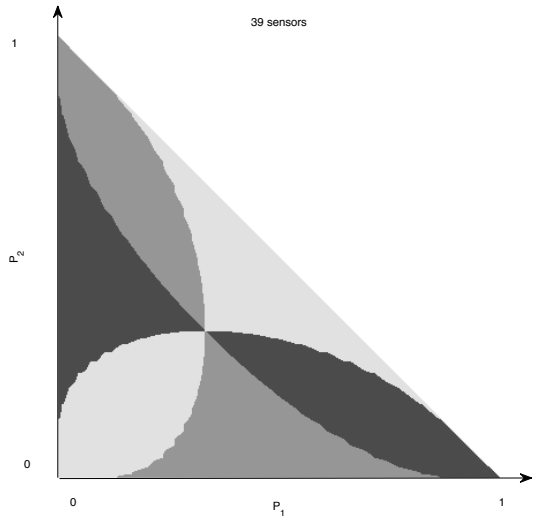

(a)

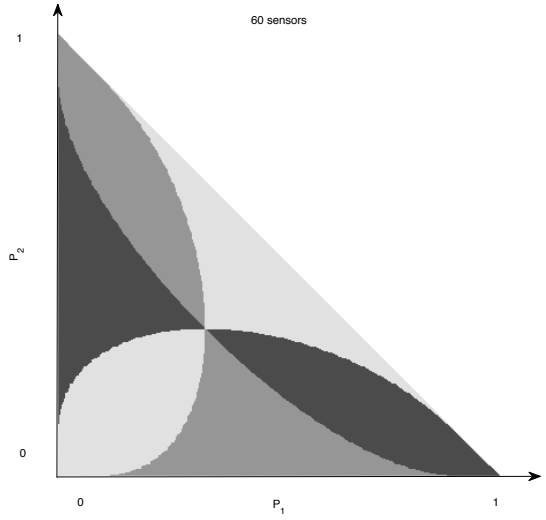

(b)

Figure 4.13: Areas identifying the best IQS. The colors of dark gray, gray and light gray respectively indicate type 1 LRQ, type 2 LRQ and type 3 LRQ gives the best IQS. The numbers of sensors in (a) and (b) are 39 and 60, respectively.

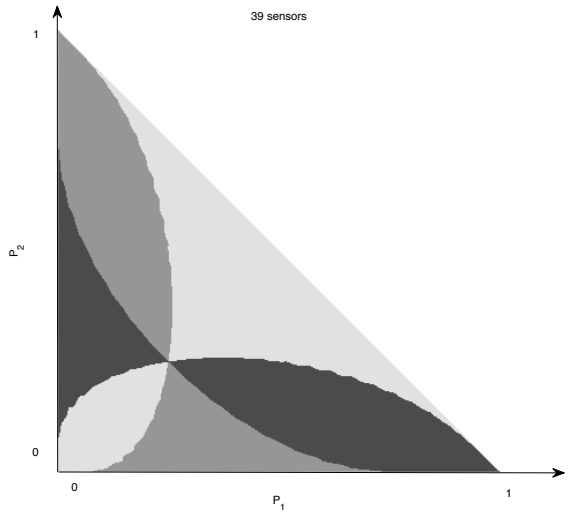

(a)

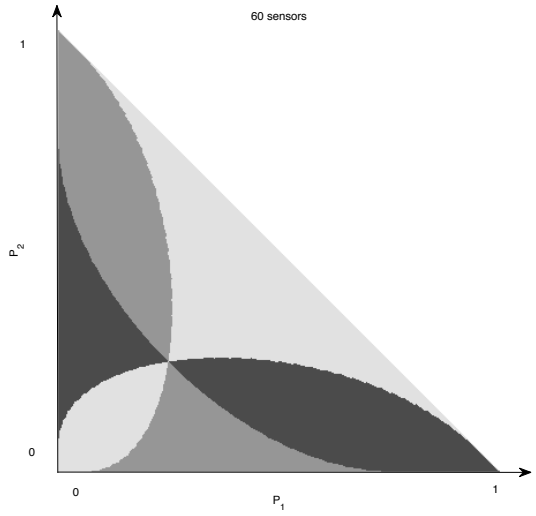

(b)

Figure 4.14: Areas identifying the best IQS. The colors of dark gray, gray and light gray respectively indicate type 1 LRQ, type 2 LRQ and type 3 LRQ gives the best IQS. The numbers of sensors in (a) and (b) are 39 and 60, respectively.

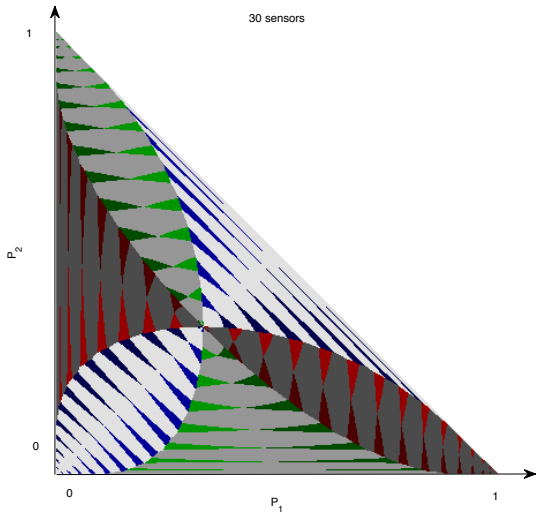

(a)

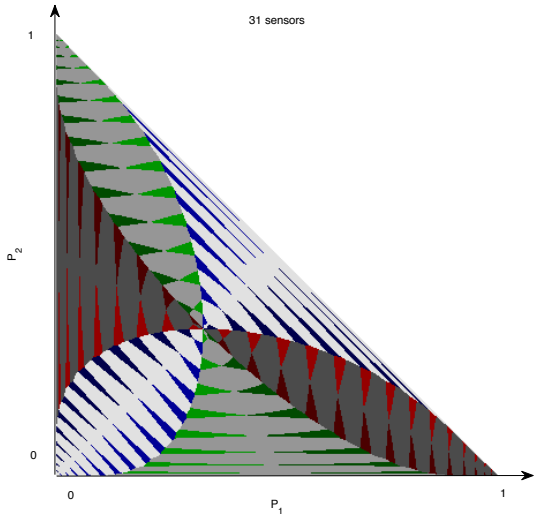

(b)

Figure 4.15: Areas that the NQS with one different LRQ outperforms the best IQS. The implications of different colors are designated in (4.1). The number of sensors are 30 and 31 for (a) and (b), respectively.

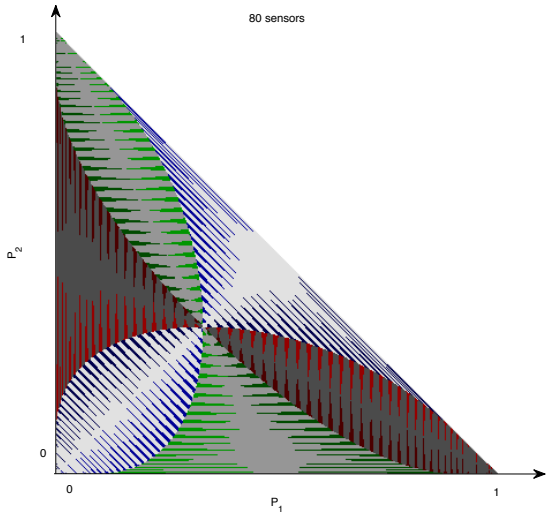

(a)

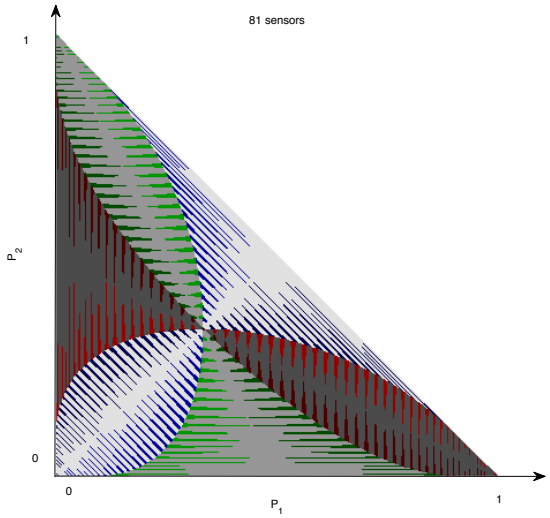

(b)

Figure 4.16: Areas that the NQS with one different LRQ outperforms the best IQS. The implications of different colors are designated in (4.1). The number of sensors are 80 and 81 for (a) and (b), respectively.

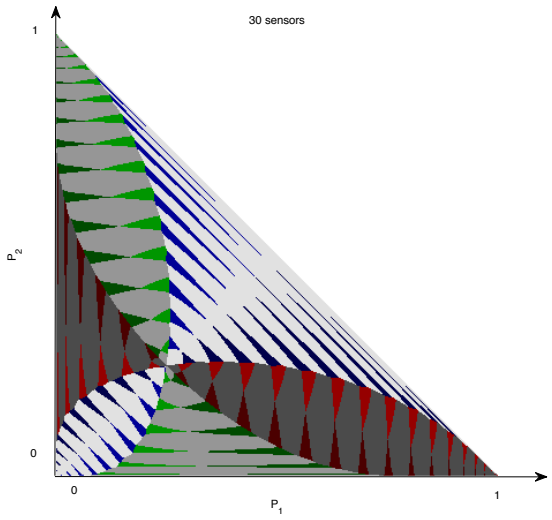

(a)

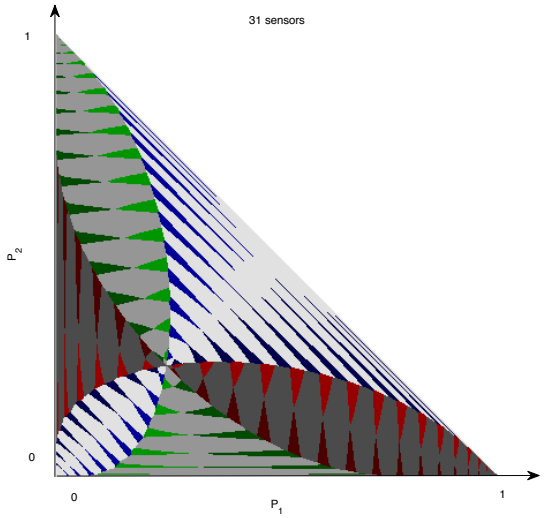

(b)

Figure 4.17: Areas that the NQS with one different LRQ outperforms the best IQS. The implications of different colors are designated in (4.1). The number of sensors are 30 and 31 for (a) and (b), respectively.

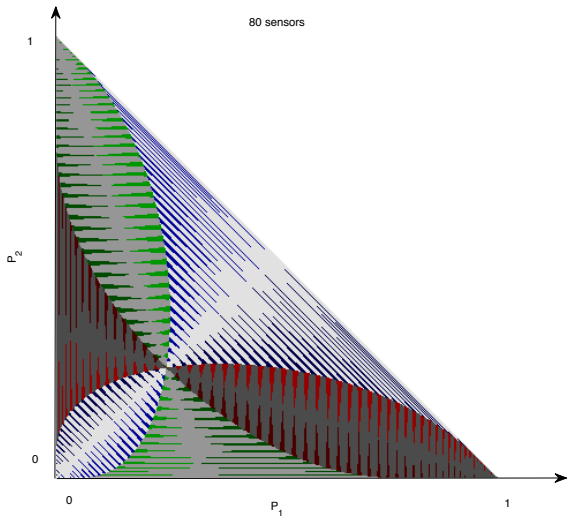

(a)

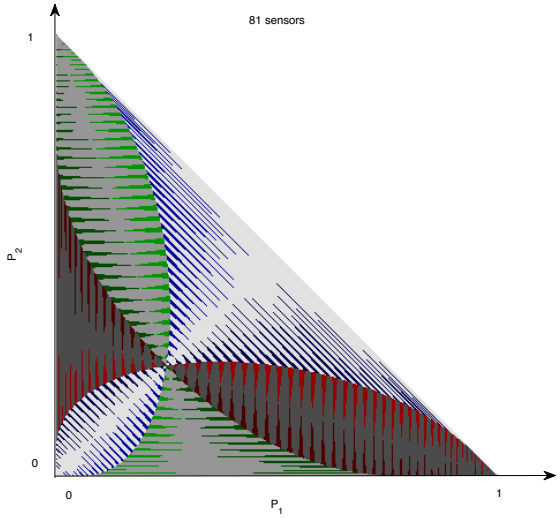

(b)

Figure 4.18: Areas that the NQS with one different LRQ outperforms the best IQS. The implications of different colors are designated in (4.1). The number of sensors are 80 and 81 for (a) and (b), respectively.

4.2 Remarks

From Figures 4.1–4.10, we observe that the best IQS is optimal in some cases but is only suboptimal in some other cases. We also note that the performance curve may not be monotonic with the number of different LRQs from the original IQS. But these curves somehow confirm the general impression that to achieve optimality in performance requires only to use very few distinct LRQs.

In order to simplify our analysis, we focus on the comparison between the best IQS and the NQS with only one distinct LRQ. To the end, we first numerically identify the best IQS in Figures 4.13 and 4.14. The following observations can be made. First, the six regions meet at the point $P_1 = P_2 = \frac{1}{3}$ in Figure 4.13 and at the point $P_1 = P_2 = \frac{1}{4}$ in Figure 4.14. Notably, at this particular point, the null hypothesis distribution is identical to the alternative hypothesis distribution. So there is no way to differentiate statistically the two hypotheses and the resulting detection errors of all designs behave equally bad. Secondly, the pattern of the six regions that identify the best IQS does not change with the total number of sensors. Thirdly, the pattern can be sub-divided into six regions of the same color.

We next test whether the NQS with one different LRQ improves the best IQS. The areas in colors other than gray show exactly the situations where the best IQS performs worse than the one-different-LRQ NQS. One can however observe that these colored areas, such as the green ones, reshape when the total number of sensors change. As the number of sensors grow, they will split into more triangular-shape bands, while these bands become slimmer. Nevertheless, one can still observe certain "symmetry" around the center point (e.g., $P_1 = P_2 = \frac{1}{3}$ in Figure 4.13) among these band patterns.

To confirm what observed in the previous paragraph can also be applied to other hy-

pothesis setting, we perform another numerical examination. The results are summarized in Figures 4.17 and 4.18. The resulting behavior of the triangular-shape bands is similar, except that the center of the symmetry of these color band patterns is changed to $P_1 = P_2 = \frac{1}{4}$. Also, the number of bands increase as the number of sensors grow; but it seems hard to determine the relation between the number of sensors and the number of narrow colored bands.

Chapter 5

Conclusion and Future Work

In this thesis, we revisit the long-standing problem in the respective literature that when the identical quantizer system (IQS) is globally optimal. Since the answer to the previous question may be hard, we alternatively ask ourselves a different but related question, i.e., when the identical quantizer system (IQS) is globally suboptimal.

By simplifying our focus on cases of ternary local observations, we found via extensive trials that the optimal design is mostly identical but uses only few (one or two) different LRQs. Based on this, we proceed to both theoretically and numerically compare the performances of the best IQS and the NQS with one different LRQ. By deriving the exact error formulas, we did locate a few line regions that the NQS outperforms the best IQS. In fact, the technique we used should be able to extend to identify a region that the NQS outperforms the best IQS, but we defer this task as a future work.

It is interesting to note from simulations that the regions that we wish to identify have some symmetry pattern around some center point. If we can prove this symmetry, then the identification of certain region could focus only on a restricted area and hence facilitate the research along this direction.

One may wish to check whether adopting two distinct LRQs, not just one, can further im-

prove the detection errors. This would be another future work that could help understanding the optimal design in a distributed detection scenario.

Bibliography

[1] Adrian Papamarcou and Po-Ning Chen, "Asymptotic refinements In Bayesian distributed detection," *1993 IEEE International Symposium on Information Theory*, Texas, USA, September 1993.

[2] J. N. Tsitsiklis, "Decentralized detection by a large number of sensors," *Mathematics of Control, Signals and Systems*,1(2):167-182, 1988.

[3] J. N. Tsitsiklis, "On threshold rules in decentralized detection," In Proc. *25th Conference on Decision and Control*, pp. 232-236, Athens, Greece, 1986.

[4] Po-Ning Chen, *Large Deviations Approaches to Performances Analysis of Distributed Detection Systems*, PH.D. thesis, University of Maryland, College Park, USA, June 1994.

[5] Ying Lin, Biao Chen, and Bruce Suter, "Robust binary quantizers for distributed detection," *IEEE Trans. Wireless Communications*, vol. 6, no. 6, June 2007.

[6] Patrick Billingsley, *Probability and Measure*, 3rd Edition, Wiley, 1995.